

## A New Class Of Quadruplex DNA-Binding Nickel Schiff Base Complexes

Son Q.T. Pham,<sup>a,b</sup> Nawal Assadawi,<sup>a,b</sup> Jadon Wells,<sup>a,b</sup> Reece A. Sophocleous,<sup>a,b,c</sup> Kimberley J. Davis,<sup>a,b</sup> Haibo Yu,<sup>a,b</sup> Ronald Sluyter,<sup>a,b,c</sup> Carolyn T. Dillon,<sup>a,b</sup> Celine Kelso,<sup>a,b</sup> Jennifer L. Beck,<sup>a,b</sup> Anthony C. Willis,<sup>d</sup> Christopher Richardson<sup>a,b</sup> and Stephen F. Ralph<sup>a,b\*</sup>

### Supplementary Material

#### Table of contents

Table S1 Crystal data and structure refinement for complex (3).....	4
Table S2 Crystal data and structure refinement for complex (4).....	6
Table S3 Crystal data and structure refinement for complex (5).....	8
Table S4 Crystal data and structure refinement for complex (6).....	10
Table S5 Crystal data and structure refinement for complex (7).....	12
Table S6 Crystal data and structure refinement for complex (8).....	14
Table S7 Crystal data and structure refinement for complex (9).....	16
Table S8 Crystal data and structure refinement for complex (13).....	18
Table S9 Hydrogen Bonds for (13). .....	19
Table S10 Crystal data and structure refinement for complex (14).....	20
Table S11 Selected bond lengths (Å), bond angles (°) and average coplanar ring angles (°) for complexes (5), (7), (9), and (13).....	22
Figure S1 The asymmetric unit of complex (3).....	5
Figure S2 The asymmetric unit of complex (4).....	7
Figure S3 The asymmetric unit of complex (5).....	9
Figure S4 The asymmetric unit of complex (6).....	11
Figure S5 The asymmetric unit of complex (7).....	13
Figure S6 The asymmetric unit of complex (8).....	15
Figure S7 The asymmetric unit of complex (9) without the acetonitrile solvates. ....	17
Figure S8 The asymmetric unit of complex (13) with only the major orientations of the methanol solvates based on C10 and C1E. ....	19
Figure S9 The asymmetric unit of complex (14).....	21
Figure S10 Relative abundances of ions in ESI mass spectra .....	23
Figure S11 Circular dichroism spectra of solutions containing different ratios of (1) and various DNA: .....	24
Figure S12 Circular dichroism spectra of solutions containing different ratios of (4) and various DNA: .....	25
Figure S13 Circular dichroism spectra of solutions containing different ratios of (6) and various DNA: .....	26
Figure S14 Circular dichroism spectra of solutions containing different ratios of (8) and various DNA: .....	27

Figure S15 Circular dichroism spectra of solutions containing different ratios of (10) and various DNA: .....	28
Figure S16 Circular dichroism spectra of solutions containing different ratios of (12) and various DNA: .....	29
Figure S17 Normalised FRET melting curves obtained using solutions containing 0.2 $\mu$ M F21T and different concentrations of (1).....	30
Figure S18 Normalised FRET melting curves obtained using solutions containing 0.2 $\mu$ M F21T and different concentrations of (4).....	30
Figure S19 Normalised FRET melting curves obtained using solutions containing 0.2 $\mu$ M F21T and different concentrations of (6).....	31
Figure S20 Normalised FRET melting curves obtained using solutions containing 0.2 $\mu$ M F21T and different concentrations of (8).....	31
Figure S21 Normalised FRET melting curves obtained using solutions containing 0.2 $\mu$ M F21T and different concentrations of (10).....	32
Figure S22 Normalised FRET melting curves obtained using solutions containing 0.2 $\mu$ M F21T and different concentrations of (12).....	32
Figure S23 Normalised FRET melting curves obtained using solutions containing 0.2 $\mu$ M F21T and different concentrations of (14).....	33
Figure S24 Fluorescence spectra for solution containing Q1 and TO upon addition of increasing amounts of complex (1).....	33
Figure S25 Fluorescence spectra for solution containing Q1 and TO upon addition of increasing amounts of complex (4).....	34
Figure S26 Fluorescence spectra for solution containing Q1 and TO upon addition of increasing amounts of complex (6).....	34
Figure S27 Fluorescence spectra for solution containing Q1 and TO upon addition of increasing amounts of complex (8).....	35
Figure S28 Fluorescence spectra for solution containing Q1 and TO upon addition of increasing amounts of complex (10).....	35
Figure S29 Fluorescence spectra for solution containing Q1 and TO upon addition of increasing amounts of complex (12).....	36
Figure S30 Fluorescence spectra for solution containing Q1 and TO upon addition of increasing amounts of complex (14).....	36
Figure S31 Stern-Volmer plots for FID assays of complexes (1), (4), (6), (8), (10), (12) and (14) using Q1 and TO.....	37
Figure S32 Molecular docking configurations of complex (1), (6), (8), (10) and (12).....	38
Figure S33 Images obtained from time course fluorescence experiments performed using of V79 cells. All images were obtained using 10x magnification. ....	39

## Crystallography

X-ray data for complexes **(4)**, **(5)**, **(7)**, **(8)** and **(14)** were collected at 150 K using a SuperNova Dual EoS2 diffractometer with Cu K $\alpha$  radiation;  $\lambda = 1.54184 \text{ \AA}$ . *CrysAlis PRO* 1.171.38.43 (Rigaku, OD, 2016) or 1.171.38.46 (Rigaku OD, 2017) were used for data collection and reduction, and cell refinement. Structures were solved by applying the full matrix least-squares method using *SIR92*,[1] and refined using *CRYSTALS*. [2] Empirical absorption corrections using special harmonics were implemented using the SCALE3 ABSPACK scaling algorithm.

X-ray data for **(3)**, **(6)**, **(9)** and **(13)** were collected at 150 K using a Rigaku XtaLAB MINI II diffractometer with Mo K $\alpha$  radiation;  $\lambda = 0.71073 \text{ \AA}$ . *CrysAlis PRO* 171.39.45f (Rigaku, OD, 2019) was used for data collection and reduction, and cell refinement. Structures were solved using *ShelXT*, [3] and refined using *ShelXL* [4] under the *OLEX*<sup>2</sup> graphical user interface. [5] Empirical absorption corrections using special harmonics were implemented using the SCALE3 ABSPACK scaling algorithm.

**Table S1** Crystal data and structure refinement for complex **(3)**.

Empirical formula	C <sub>32</sub> H <sub>22</sub> D <sub>12</sub> N <sub>2</sub> NiO <sub>6</sub> S <sub>2</sub>
Formula weight	677.51
Temperature/K	150.00(10)
Crystal system	monoclinic
Space group	<i>P</i> 2 <sub>1</sub> / <i>n</i>
<i>a</i> /Å	16.4100(2)
<i>b</i> /Å	9.8299(2)
<i>c</i> /Å	21.9572(5)
$\alpha$ /°	90
$\beta$ /°	100.1632(18)
$\gamma$ /°	90
Volume/Å <sup>3</sup>	3486.30(13)
<i>Z</i>	4
$\rho_{\text{calc}}$ /g/cm <sup>3</sup>	1.291
$\mu$ /mm <sup>-1</sup>	0.718
<i>F</i> (000)	1392.0
Crystal size/mm <sup>3</sup>	0.5 × 0.4 × 0.1
Radiation	MoK $\alpha$ ( $\lambda$ = 0.71073)
2 $\theta$ range for data collection/°	3.404 to 57.4
Index ranges	-22 ≤ <i>h</i> ≤ 22, -13 ≤ <i>k</i> ≤ 13, -29 ≤ <i>l</i> ≤ 29
Reflections collected	64412
Independent reflections	8956 [ <i>R</i> <sub>int</sub> = 0.0326, <i>R</i> <sub>sigma</sub> = 0.0203]
Data/restraints/parameters	8956/2/418
Goodness-of-fit on <i>F</i> <sup>2</sup>	1.022
Final <i>R</i> indexes [ <i>I</i> ≥ 2 $\sigma$ ( <i>I</i> )]	<i>R</i> <sub>1</sub> = 0.0329, <i>wR</i> <sub>2</sub> = 0.0862
Final <i>R</i> indexes [all data]	<i>R</i> <sub>1</sub> = 0.0389, <i>wR</i> <sub>2</sub> = 0.0895
Largest diff. peak/hole / e Å <sup>-3</sup>	1.21/-0.41

Compound **(3)** crystallised from a solution of deuterated dimethylsulfoxide with one full complex and two solvent molecules, one of which is disordered, in the asymmetric unit. The disordered DMSO was modelled via a free variable (ratio 82:18) with S-O and S-C distance restraints to make the minor occupancy molecule sensible. A shared site {C1AA, C501} was constrained with equivalent displacement parameters. The methyl groups were refined as rotating groups and converged. There is one large positive peak in the difference map between the sulfur atoms of the disordered deuterated DMSO molecules. This is perhaps indicative of a third position in the disorder model. Attempted modelling of this lead to no better model for refinement.

All hydrogens were placed in calculated positions and allowed to ride on their carrier atoms with fixed *U*iso values (C(H) and C(H,H) groups at 1.2 times; C(H,H,H) groups and O(H)

groups at 1.5 times). The idealised hydrogens attached to oxygen were refined as freely rotating and led to the hydrogen bonding displayed in Figure S1.

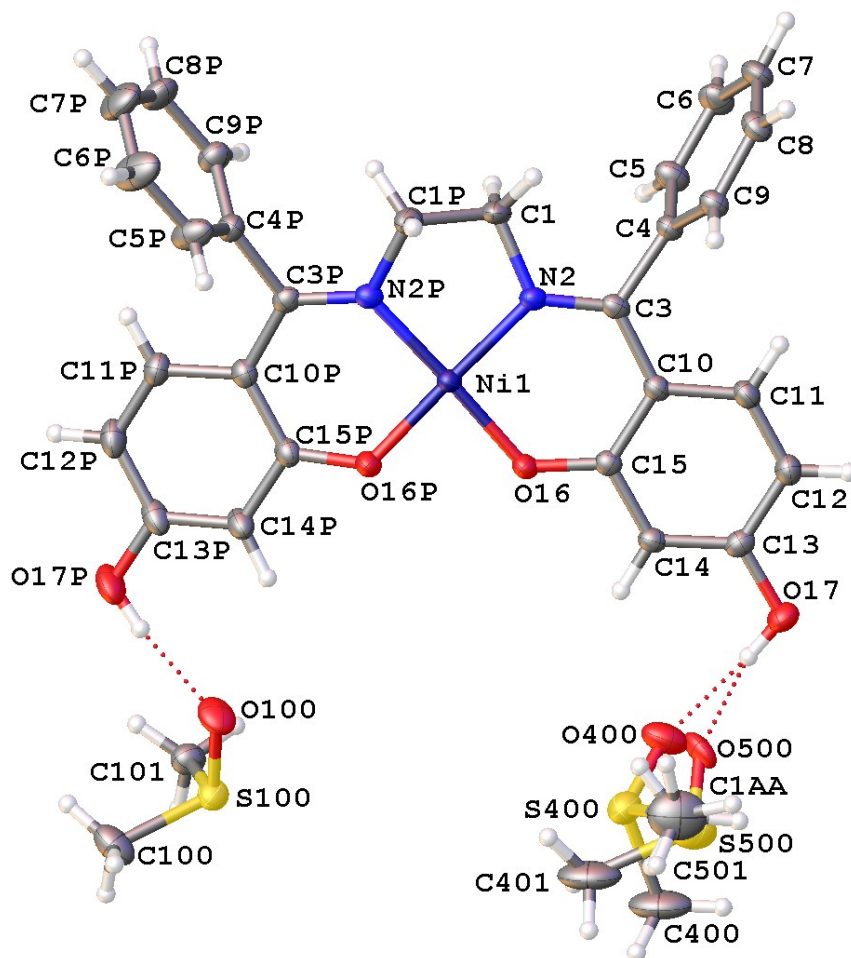


**Figure S1** The asymmetric unit of complex (3).

**Table S2** Crystal data and structure refinement for complex **(4)**.

Empirical formula	C <sub>42</sub> H <sub>48</sub> N <sub>4</sub> NiO <sub>4</sub>
Formula weight	731.58
Temperature/K	150
Crystal system	monoclinic
Space group	<i>P</i> 2 <sub>1</sub> / <i>c</i>
<i>a</i> /Å	15.6742(16)
<i>b</i> /Å	9.0717(8)
<i>c</i> /Å	26.436(3)
$\alpha$ /°	90
$\beta$ /°	94.398(9)
$\gamma$ /°	90
Volume/Å <sup>3</sup>	3747.9(7)
<i>Z</i>	4
$\rho_{\text{calc}}$ /g/cm <sup>3</sup>	1.296
$\mu$ /mm <sup>-1</sup>	1.118
<i>F</i> (000)	1552.0
Crystal size/mm <sup>3</sup>	0.122 × 0.076 × 0.021
Radiation	Cu K $\alpha$ ( $\lambda$ = 1.54184)
2 $\theta$ range for data collection/°	8.438 to 143.672
Index ranges	-19 ≤ <i>h</i> ≤ 18, -7 ≤ <i>k</i> ≤ 11, -32 ≤ <i>l</i> ≤ 29
Reflections collected	24063
Independent reflections	7203 [ <i>R</i> <sub>int</sub> = 0.074]
Data/restraints/parameters	7203/109/542
Goodness-of-fit on <i>F</i> <sup>2</sup>	0.953
Final <i>R</i> indexes [ <i>I</i> ≥ 2 $\sigma$ ( <i>I</i> )]	<i>R</i> <sub>1</sub> = 0.0810, <i>wR</i> <sub>2</sub> = 0.1717
Final <i>R</i> indexes [all data]	<i>R</i> <sub>1</sub> = 0.1307, <i>wR</i> <sub>2</sub> = 0.2019
Largest diff. peak/hole / e Å <sup>-3</sup>	0.70/-0.59

The crystals of **(4)** which were supplied were very thin and flaky. A segment was eventually found which gave weak diffraction but appeared to be largely single. The final *R*-factor is poor but the identity of the compound is unambiguously established. There is disorder in the packing of one arm of the **(4)** molecule. Atoms O4, N4 and C36 — C42 are each disordered over two sites. The relative occupancies of these sites were refined appropriately. Restraints were imposed so bond lengths and angles would have sensible values, and so adjacent sites would have similar displacement parameters to each other. H atoms were included at calculated positions and ride on the C atom sites to which they are respectively bonded. The largest features in the final difference electron density map are located randomly through the structure including near the Ni atom and near atoms C19 — C23 possibly indicating a small amount of disorder of the packing of this group too.

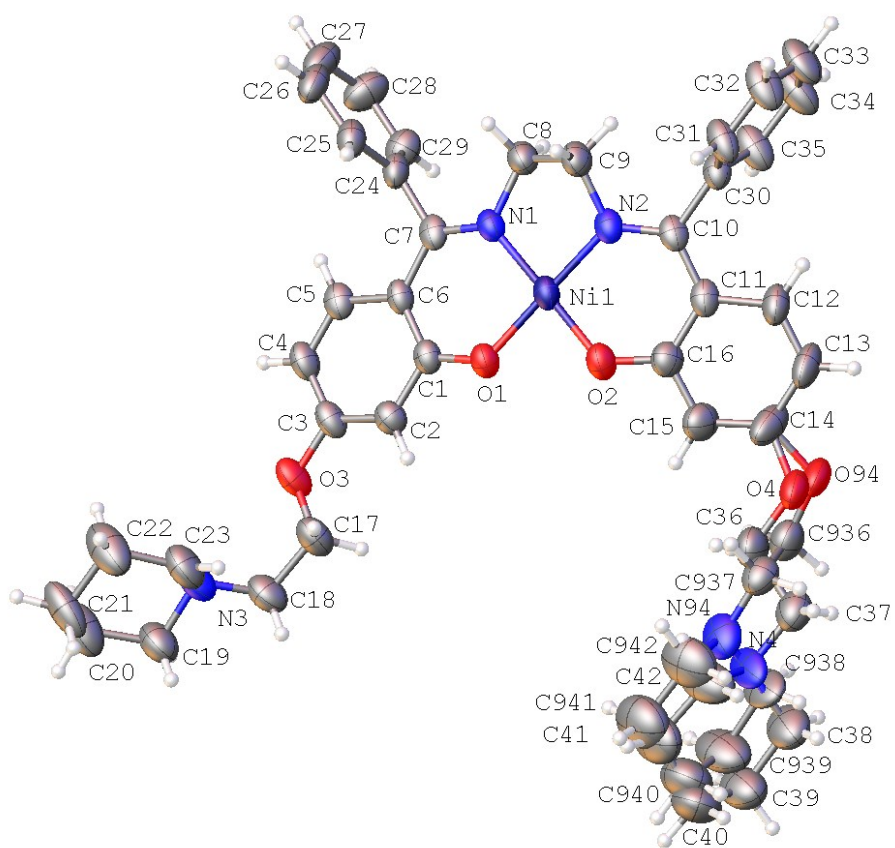


**Figure S2** The asymmetric unit of complex **(4)**.

**Table S3** Crystal data and structure refinement for complex **(5)**.

Empirical formula	C <sub>33</sub> H <sub>38</sub> N <sub>2</sub> NiO <sub>7</sub> S <sub>2</sub>
Formula weight	697.52
Temperature/K	150
Crystal system	triclinic
Space group	$P\bar{1}$
a/Å	9.9443(2)
b/Å	10.8213(2)
c/Å	15.0907(3)
$\alpha$ /°	90.9180(16)
$\beta$ /°	95.2472(16)
$\gamma$ /°	94.9377(15)
Volume/Å <sup>3</sup>	1610.64(5)
Z	2
$\rho_{\text{calc}}/\text{g}/\text{cm}^3$	1.438
$\mu/\text{mm}^{-1}$	2.504
F(000)	732.0
Crystal size/mm <sup>3</sup>	0.292 × 0.112 × 0.065
Radiation	Cu K $\alpha$ ( $\lambda$ = 1.54184)
2 $\theta$ range for data collection/°	5.882 to 147.676
Index ranges	-11 ≤ h ≤ 12, -13 ≤ k ≤ 13, -17 ≤ l ≤ 18
Reflections collected	32422
Independent reflections	6529 [R <sub>int</sub> = 0.019]
Data/restraints/parameters	6529/33/451
Goodness-of-fit on F <sup>2</sup>	1.008
Final R indexes [I >= 2 $\sigma$ (I)]	R <sub>1</sub> = 0.0383, wR <sub>2</sub> = 0.0967
Final R indexes [all data]	R <sub>1</sub> = 0.0388, wR <sub>2</sub> = 0.0970
Largest diff. peak/hole / e Å <sup>-3</sup>	1.07/-0.92

Complex **(5)** is the racemic mixture of two enantiomers. As a consequence, there is disorder in the packing of the **(5)** molecules so the methyl group appears to be attached to either C8 or C9. Two sites were used for each of C8, C9 and C23 (the corresponding sites being named C98, C99 and C923). Methyl C23 is bonded to C8, whereas C923 is bonded to C99. The relative occupancies of these sites were refined appropriately. Restraints were imposed so corresponding bond lengths should tend to be equal and so adjacent sites would have similar displacement parameters to each other.

A subsequent difference electron map showed a peak close to S1 which suggested that this dimethylsulfoxide molecule was disordered to a small extent, with the 2 C atoms and O atom being common to each orientation, but with S atom sites on each side of the plane described by those atoms. This additional S site was included with an isotropic displacement

parameter and the relative occupancies of the *S* sites were refined. Restraints were applied so *S*—*X* distances for the minor *S* site would tend towards expected values.

H atoms away from the disorder were observed in a difference map and those bonded to C were positioned geometrically. The H atoms away from the disorder were initially refined with soft restraints on the bond lengths and angles to regularize their geometry (C—H in the range 0.93–0.98 Å, O—H = 0.83 Å) and with *U*<sub>iso</sub>(H) in the range 1.2–1.5 times *U*<sub>eq</sub> of the parent atom, after which the positions were refined with riding constraints and the displacement parameters were held fixed. Finally the positions of the H atoms bonded to O were allowed to refine with distance restraints. H atoms of the disordered atoms were maintained at calculated positions and ride on the C atom sites to which they are respectively bonded. The largest features in the final difference electron density map are located near the Ni atom and within the disordered parts of the structure.

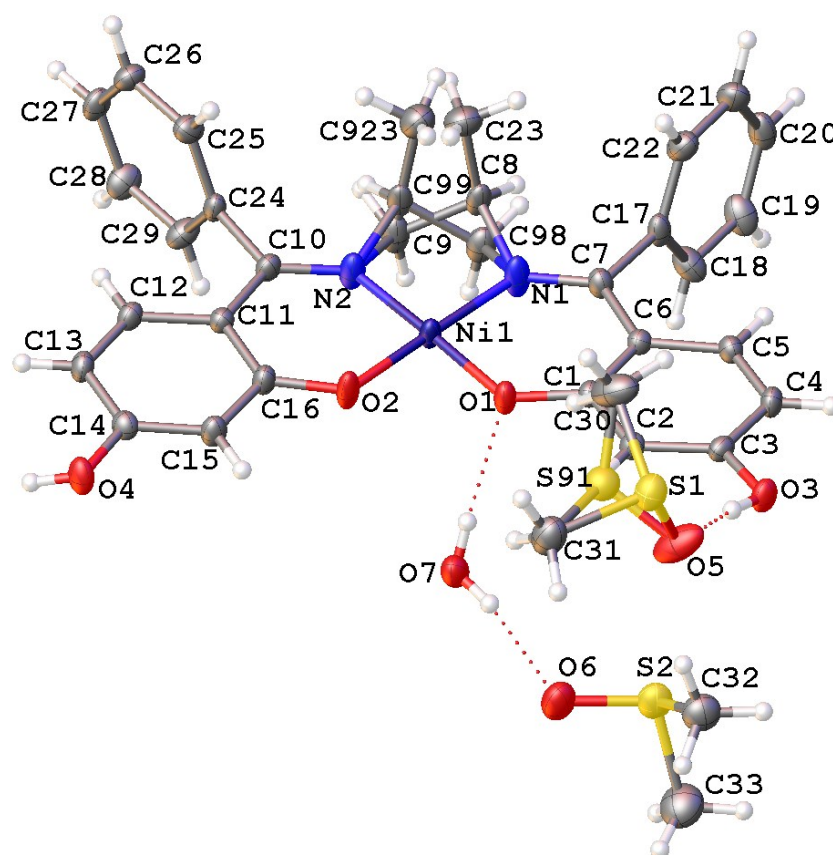


**Figure S3** The asymmetric unit of complex (5).

**Table S4** Crystal data and structure refinement for complex (6).

Empirical formula	C <sub>43</sub> H <sub>50</sub> N <sub>4</sub> NiO <sub>4</sub>
Formula weight	745.58
Temperature/K	149.99(10)
Crystal system	triclinic
Space group	$P\bar{1}$
a/Å	11.83480(19)
b/Å	12.9908(2)
c/Å	16.1427(3)
$\alpha$ /°	67.3813(17)
$\beta$ /°	74.2421(15)
$\gamma$ /°	79.8434(15)
Volume/Å <sup>3</sup>	2197.62(7)
Z	2
$\rho_{\text{calc}}/\text{g}/\text{cm}^3$	1.127
$\mu/\text{mm}^{-1}$	0.483
F(000)	792.0
Crystal size/mm <sup>3</sup>	0.41 × 0.26 × 0.19
Radiation	MoK $\alpha$ ( $\lambda$ = 0.71073)
2 $\theta$ range for data collection/°	3.408 to 54.204
Index ranges	-14 ≤ h ≤ 15, -16 ≤ k ≤ 16, -20 ≤ l ≤ 20
Reflections collected	48728
Independent reflections	9563 [ $R_{\text{int}}$ = 0.0232, $R_{\text{sigma}}$ = 0.0200]
Data/restraints/parameters	9563/76/536
Goodness-of-fit on F <sup>2</sup>	1.071
Final R indexes [ $I \geq 2\sigma(I)$ ]	$R_1$ = 0.0354, $wR_2$ = 0.0965
Final R indexes [all data]	$R_1$ = 0.0429, $wR_2$ = 0.1000
Largest diff. peak/hole / e Å <sup>-3</sup>	0.29/-0.25

The compound crystallises with a full complex and a molecule of hexane in the asymmetric unit. The hexane was disordered and a satisfactory model was not derived and so it was removed using Bypass. One of the piperidinyll rings (N18-C23) is disordered over 2 positions and was modelled as two-component disorder (ratio 68:32) using the same fragment (N18-C23) as a rotatable rigid group along with a RIGU restraint. The nitrogen atom is common to both orientations and the displacement parameters were constrained to be the same.

The disorder about the ethylenediamine backbone was modelled as two-component disorder (ratio 85:15) with DFIX restraints for the minor component (N1-C2P C2P-C1P C1P-N3 C1P-C1MP).

All hydrogen atom positions were idealised and refined with riding coordinates with fixed Uiso (CH and CH<sub>2</sub> groups at 1.2 times their carrier atoms and CH<sub>3</sub> groups at 1.5 times their carrier atoms). The CH<sub>3</sub> groups were refined as rotating groups.

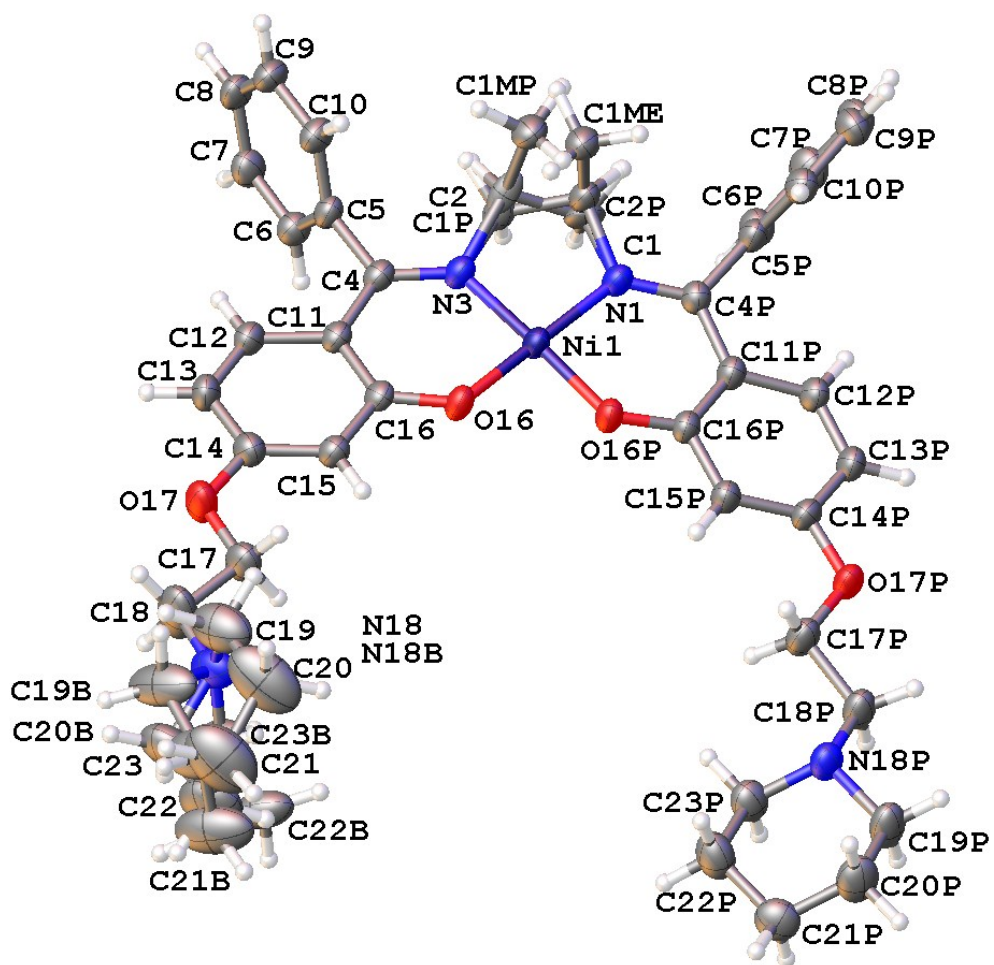


**Figure S4** The asymmetric unit of complex (6).

**Table S5** Crystal data and structure refinement for complex **(7)**.

Empirical formula	C <sub>31</sub> H <sub>36</sub> N <sub>2</sub> NiO <sub>8</sub> S
Formula weight	655.41
Temperature/K	150
Crystal system	Monoclinic
Space group	<i>P2<sub>1</sub>/n</i>
<i>a</i> /Å	12.8742(1)
<i>b</i> /Å	9.3175(1)
<i>c</i> /Å	25.5985(2)
$\alpha$ /°	90
$\beta$ /°	98.4790(7)
$\gamma$ /°	90
Volume/Å <sup>3</sup>	3037.11(5)
<i>Z</i>	4
$\rho_{\text{calc}}$ /g/cm <sup>3</sup>	1.433
$\mu$ /mm <sup>-1</sup>	2.018
<i>F</i> (000)	1376.0
Crystal size/mm <sup>3</sup>	0.187 × 0.133 × 0.092
Radiation	Cu K $\alpha$ ( $\lambda$ = 1.54184)
2 $\theta$ range for data collection/°	6.982 to 147.702
Index ranges	-16 ≤ <i>h</i> ≤ 15, -11 ≤ <i>k</i> ≤ 11, -31 ≤ <i>l</i> ≤ 28
Reflections collected	44751
Independent reflections	6155 [ <i>R</i> <sub>int</sub> = 0.027]
Data/restraints/parameters	6155/3/413
Goodness-of-fit on <i>F</i> <sup>2</sup>	0.996
Final <i>R</i> indexes [ <i>I</i> ≥ 2 $\sigma$ ( <i>I</i> )]	<i>R</i> <sub>1</sub> = 0.0298, <i>wR</i> <sub>2</sub> = 0.0783
Final <i>R</i> indexes [all data]	<i>R</i> <sub>1</sub> = 0.0313, <i>wR</i> <sub>2</sub> = 0.0794
Largest diff. peak/hole / e Å <sup>-3</sup>	0.37/-0.26

The H atoms were all located in a difference map, but those bonded to C were repositioned geometrically. The H atoms were initially refined with soft restraints on the bond lengths and angles to regularize their geometry (C—H in the range 0.93–0.98 Å, O—H = 0.83 Å) and with *U*<sub>iso</sub>(H) in the range 1.2–1.5 times *U*<sub>eq</sub> of the parent atom, after which the positions were refined with riding constraints and the displacement parameters were held fixed. Finally the positions of the H atoms bonded to O were also allowed to refine freely, but with restraints on O—H angle and H—O—H angle for O8 only. The largest features in the final difference electron density map are located near O8 and then midway between bonded C atoms. The former might suggest some disorder in the H atom positions about O8.

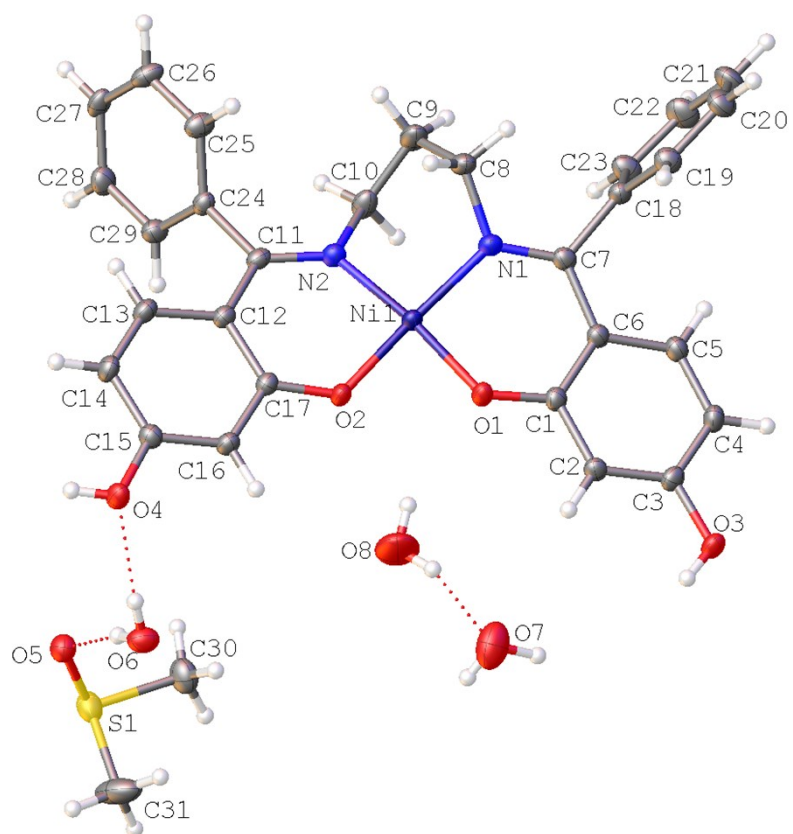


**Figure S5** The asymmetric unit of complex **(7)**.

**Table S6** Crystal data and structure refinement for complex **(8)**.

Empirical formula	C <sub>44</sub> H <sub>52</sub> Cl <sub>2</sub> N <sub>4</sub> NiO <sub>4</sub>
Formula weight	830.54
Temperature/K	150
Crystal system	monoclinic
Space group	<i>P</i> 2 <sub>1</sub> / <i>c</i>
<i>a</i> /Å	14.6486(1)
<i>b</i> /Å	8.8879(1)
<i>c</i> /Å	31.2974(3)
$\alpha$ /°	90
$\beta$ /°	91.8126(8)
$\gamma$ /°	90
Volume/Å <sup>3</sup>	4072.74(7)
<i>Z</i>	4
$\rho_{\text{calc}}$ /g/cm <sup>3</sup>	1.354
$\mu$ /mm <sup>-1</sup>	2.272
<i>F</i> (000)	1752.0
Crystal size/mm <sup>3</sup>	0.356 × 0.078 × 0.018
Radiation	Cu K $\alpha$ ( $\lambda$ = 1.54184)
2 $\theta$ range for data collection/°	6.036 to 147.598
Index ranges	-18 ≤ <i>h</i> ≤ 18, -11 ≤ <i>k</i> ≤ 8, -38 ≤ <i>l</i> ≤ 38
Reflections collected	61919
Independent reflections	8211 [ <i>R</i> <sub>int</sub> = 0.032]
Data/restraints/parameters	8211/0/496
Goodness-of-fit on <i>F</i> <sup>2</sup>	0.996
Final <i>R</i> indexes [ <i>I</i> ≥ 2 $\sigma$ ( <i>I</i> )]	<i>R</i> <sub>1</sub> = 0.0522, <i>wR</i> <sub>2</sub> = 0.1360
Final <i>R</i> indexes [all data]	<i>R</i> <sub>1</sub> = 0.0556, <i>wR</i> <sub>2</sub> = 0.1397
Largest diff. peak/hole / e Å <sup>-3</sup>	0.89/-1.54

The H atoms were all located in a difference map, but were repositioned geometrically. The H atoms were initially refined with soft restraints on the bond lengths and angles to regularize their geometry (C—H in the range 0.93–0.98 Å) and with *U*<sub>iso</sub>(H) in the range 1.2–1.5 times *U*<sub>eq</sub> of the parent atom, after which the positions were refined with riding constraints and the displacement parameters were held fixed. The largest features in the final difference electron density map are located near the Cl atoms of the solvate and then midway between bonded C atoms. The former might suggest some disorder of solvate molecules with the possible presence of acetone or water instead of dichloromethane.

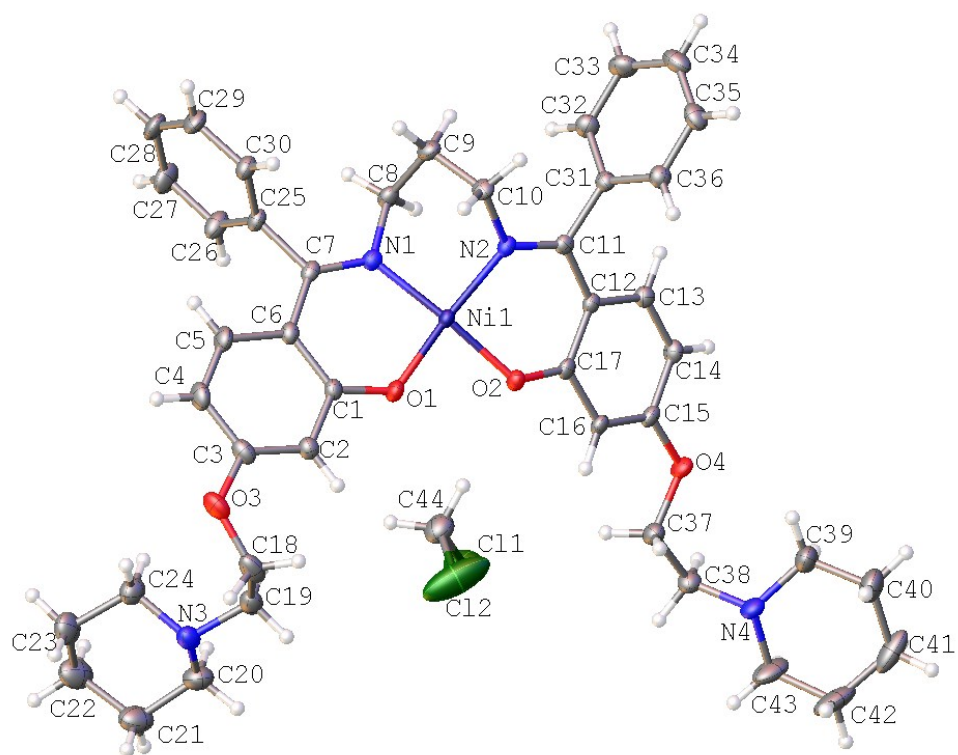


**Figure S6** The asymmetric unit of complex **(8)**.

**Table S7** Crystal data and structure refinement for complex **(9)**.

Empirical formula	C <sub>33</sub> H <sub>34</sub> N <sub>4</sub> NiO <sub>7</sub>
Formula weight	657.35
Temperature/K	149.99(10)
Crystal system	monoclinic
Space group	<i>P</i> 2 <sub>1</sub> / <i>n</i>
<i>a</i> /Å	18.3041(4)
<i>b</i> /Å	8.07129(16)
<i>c</i> /Å	21.2716(4)
$\alpha$ /°	90
$\beta$ /°	100.144(2)
$\gamma$ /°	90
Volume/Å <sup>3</sup>	3093.50(11)
<i>Z</i>	4
$\rho_{\text{calc}}$ /g/cm <sup>3</sup>	1.411
$\mu$ /mm <sup>-1</sup>	0.682
<i>F</i> (000)	1376.0
Crystal size/mm <sup>3</sup>	0.35 × 0.15 × 0.05
Radiation	MoK $\alpha$ ( $\lambda$ = 0.71073)
2 $\theta$ range for data collection/°	5.41 to 57.398
Index ranges	-24 ≤ <i>h</i> ≤ 24, -10 ≤ <i>k</i> ≤ 10, -26 ≤ <i>l</i> ≤ 28
Reflections collected	48656
Independent reflections	7953 [ <i>R</i> <sub>int</sub> = 0.0386, <i>R</i> <sub>sigma</sub> = 0.0342]
Data/restraints/parameters	7953/54/447
Goodness-of-fit on <i>F</i> <sup>2</sup>	1.026
Final <i>R</i> indexes [ <i>I</i> ≥ 2 $\sigma$ ( <i>I</i> )]	<i>R</i> <sub>1</sub> = 0.0448, <i>wR</i> <sub>2</sub> = 0.1041
Final <i>R</i> indexes [all data]	<i>R</i> <sub>1</sub> = 0.0617, <i>wR</i> <sub>2</sub> = 0.1109
Largest diff. peak/hole / e Å <sup>-3</sup>	0.64/-0.56

The asymmetric unit of this structure contains a complete complex of **(9)**, two water molecules and two acetonitrile molecules, one of which is disordered (ratio 62:38). All acetonitriles required fixing the C-N and C-C distances (1.15 and 1.46 Å, respectively) and isotropic restraints. The molecules are linear and they are left in the refinement with large displacement parameters. The methyl group hydrogens were idealised and refined as rotating groups riding on their carrier carbon atoms with displacement parameters 1.5 times these atoms.

The solvate water molecules were initially refined with idealized hydrogen placement to give an acceptable geometry and in the final stages were changed to rigid but rotatable groups.

The disorder in the backbone of the chelate ring was modelled via a free variable (59:41). All hydrogen atoms attached to carbon were placed in calculated positions and allowed to ride on their carrier atoms with fixed *U*iso displacements at 1.2 times for all CH and CH<sub>2</sub> groups.

The phenolic O-H hydrogens were idealised and refined as rotating groups.

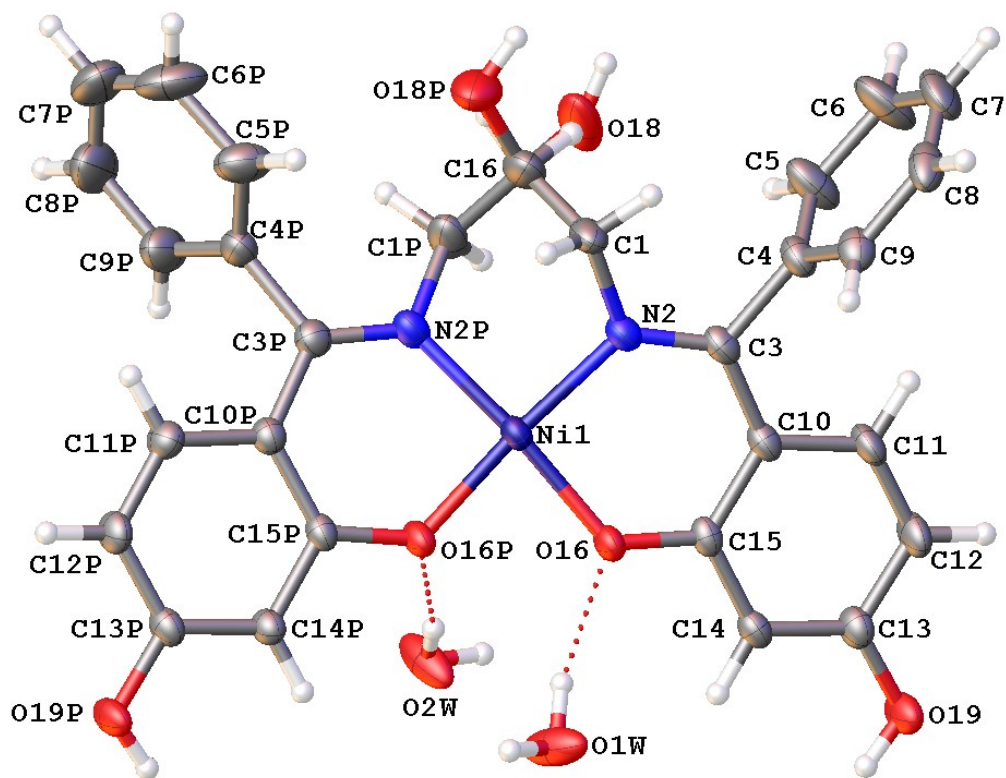


**Figure S7** The asymmetric unit of complex (9) without the acetonitrile solvates.

**Table S8** Crystal data and structure refinement for complex **(13)**.

Empirical formula	C <sub>32</sub> H <sub>38</sub> N <sub>2</sub> NiO <sub>10</sub>
Formula weight	669.35
Temperature/K	150.00(10)
Crystal system	monoclinic
Space group	<i>P2<sub>1</sub>/n</i>
a/Å	12.9739(3)
b/Å	18.8657(3)
c/Å	13.1912(2)
α/°	90
β/°	97.9782(17)
γ/°	90
Volume/Å <sup>3</sup>	3197.46(10)
Z	4
ρ <sub>calc</sub> /g/cm <sup>3</sup>	1.390
μ/mm <sup>-1</sup>	0.666
F(000)	1408.0
Crystal size/mm <sup>3</sup>	0.5 × 0.37 × 0.28
Radiation	MoKα (λ = 0.71073)
2θ range for data collection/°	3.792 to 58.258
Index ranges	-17 ≤ h ≤ 17, -25 ≤ k ≤ 25, -18 ≤ l ≤ 17
Reflections collected	44690
Independent reflections	8605 [R <sub>int</sub> = 0.0280, R <sub>sigma</sub> = 0.0231]
Data/restraints/parameters	8605/4/450
Goodness-of-fit on F <sup>2</sup>	1.034
Final R indexes [I ≥ 2σ (I)]	R <sub>1</sub> = 0.0388, wR <sub>2</sub> = 0.1067
Final R indexes [all data]	R <sub>1</sub> = 0.0474, wR <sub>2</sub> = 0.1117
Largest diff. peak/hole / e Å <sup>-3</sup>	0.88/-0.49

The structure crystallises with one metal complex and four hydrogen-bonded methanol molecules in the asymmetric unit in the space group *P2<sub>1</sub>/n*. Many of the hydrogen atoms were found in Fourier maps but all were idealized and allowed to ride on their carrier atoms and, where appropriate, refined as rotatable groups. The hydrogen-bond placements converged satisfactorily. A table of the distances and angles are provided below.

The largest residual peak (0.88 e Å<sup>-3</sup>) is 1.656 Å from C10 and may indicate an alternative orientation but no sensible modelling of this benefitted the model.

**Table S9** Hydrogen Bonds for **(13)**.

D	H	A	d(D-H)/Å	d(H-A)/Å	d(D-A)/Å	D-H-A/°
O(3)	H(3)	O(1E)	0.84	1.86	2.685(3)	167.7
O(3)	H(3)	O(1F)	0.84	1.91	2.66(2)	149.3
O(4)	H(4)	O(5) <sup>1</sup>	0.84	1.89	2.711(2)	164.5
O(5)	H(5)	O(1H)	0.84	1.74	2.555(2)	164.5
O(6)	H(6)	O(10)	0.84	1.82	2.653(6)	174.8
O(6)	H(6)	O(10B)	0.84	1.73	2.551(18)	165.8
O(1E)	H(1E)	O(6) <sup>2</sup>	0.84	1.92	2.760(3)	178.2
O(10)	H(10)	O(2) <sup>2</sup>	0.84	1.96	2.791(6)	171.8
O(1M)	H(1M)	O(3)	0.86	2.03	2.861(3)	160.8
O(1H)	H(1H)	O(1) <sup>3</sup>	0.84	1.97	2.7528(19)	154.3
O(1F)	H(1F)	O(6) <sup>2</sup>	0.84	1.98	2.778(14)	157.8
O(10B)	H(10B)	O(2) <sup>2</sup>	0.84	2.06	2.89(3)	167.0

<sup>1</sup>-X,1-Y,1-Z; <sup>2</sup>1-X,-Y,1-Z; <sup>3</sup>-1+X,+Y,+Z

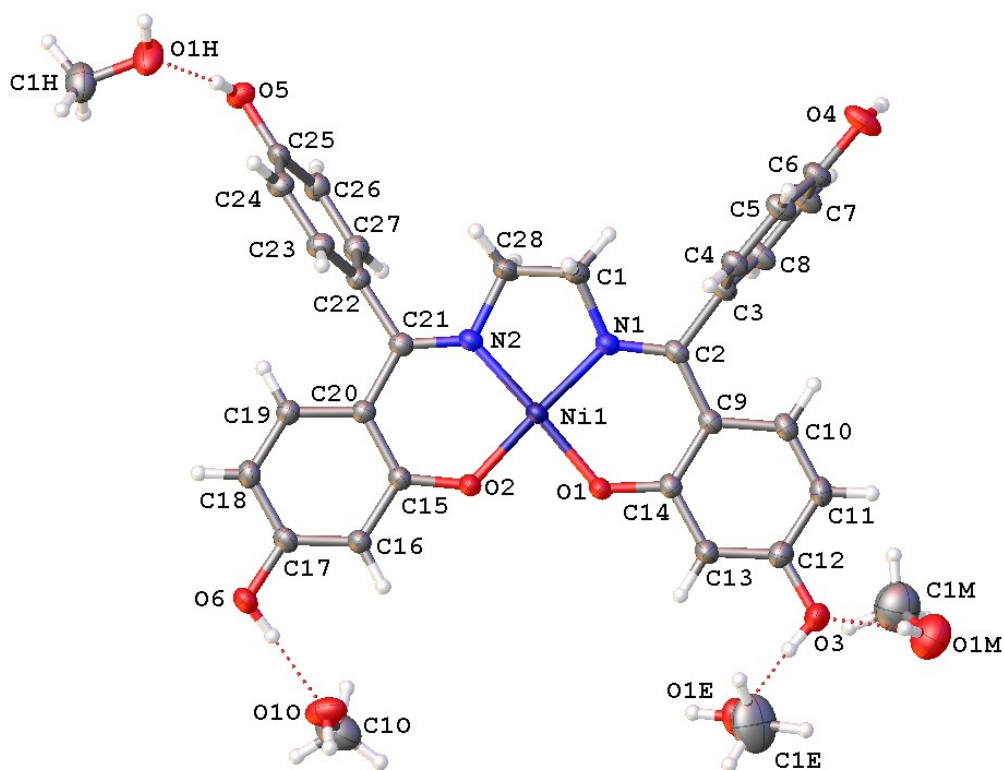


**Figure S8** The asymmetric unit of complex **(13)** with only the major orientations of the methanol solvates based on C10 and C1E.

**Table S10** Crystal data and structure refinement for complex **(14)**.

Empirical formula	C <sub>56</sub> H <sub>74</sub> N <sub>6</sub> NiO <sub>6</sub>
Formula weight	985.95
Temperature/K	150
Crystal system	triclinic
Space group	$P\bar{1}$
a/Å	10.5477(5)
b/Å	15.4745(6)
c/Å	16.5986(8)
$\alpha$ /°	88.093(3)
$\beta$ /°	83.802(4)
$\gamma$ /°	70.576(4)
Volume/Å <sup>3</sup>	2540.1(2)
Z	2
$\rho_{\text{calc}}/\text{g}/\text{cm}^3$	1.289
$\mu/\text{mm}^{-1}$	1.00
F(000)	1056
Crystal size/mm <sup>3</sup>	0.298 × 0.195 × 0.025
Radiation	Cu K $\alpha$ ( $\lambda$ = 1.54184)
2 $\theta$ range for data collection/°	6.056 to 147.786
Index ranges	-12 ≤ h ≤ 11, -19 ≤ k ≤ 18, -20 ≤ l ≤ 20
Reflections collected	28016
Independent reflections	9968 [R <sub>int</sub> = 0.054]
Data/restraints/parameters	9968/0/622
Goodness-of-fit on F <sup>2</sup>	0.964
Final R indexes [I ≥ 2 $\sigma$ (I)]	R <sub>1</sub> = 0.0638, wR <sub>2</sub> = 0.1534
Final R indexes [all data]	R <sub>1</sub> = 0.0910, wR <sub>2</sub> = 0.1766
Largest diff. peak/hole / e Å <sup>-3</sup>	0.77/-0.63

The H atoms were all located in a difference map, but were repositioned geometrically. The H atoms were initially refined with soft restraints on the bond lengths and angles to regularize their geometry (C—H in the range 0.93–0.98 Å) and with  $U_{\text{iso}}(\text{H})$  in the range 1.2–1.5 times  $U_{\text{eq}}$  of the parent atom, after which the positions were refined with riding constraints and the displacement parameters were held fixed. The largest features in the final difference electron density map are located near the Ni atom.

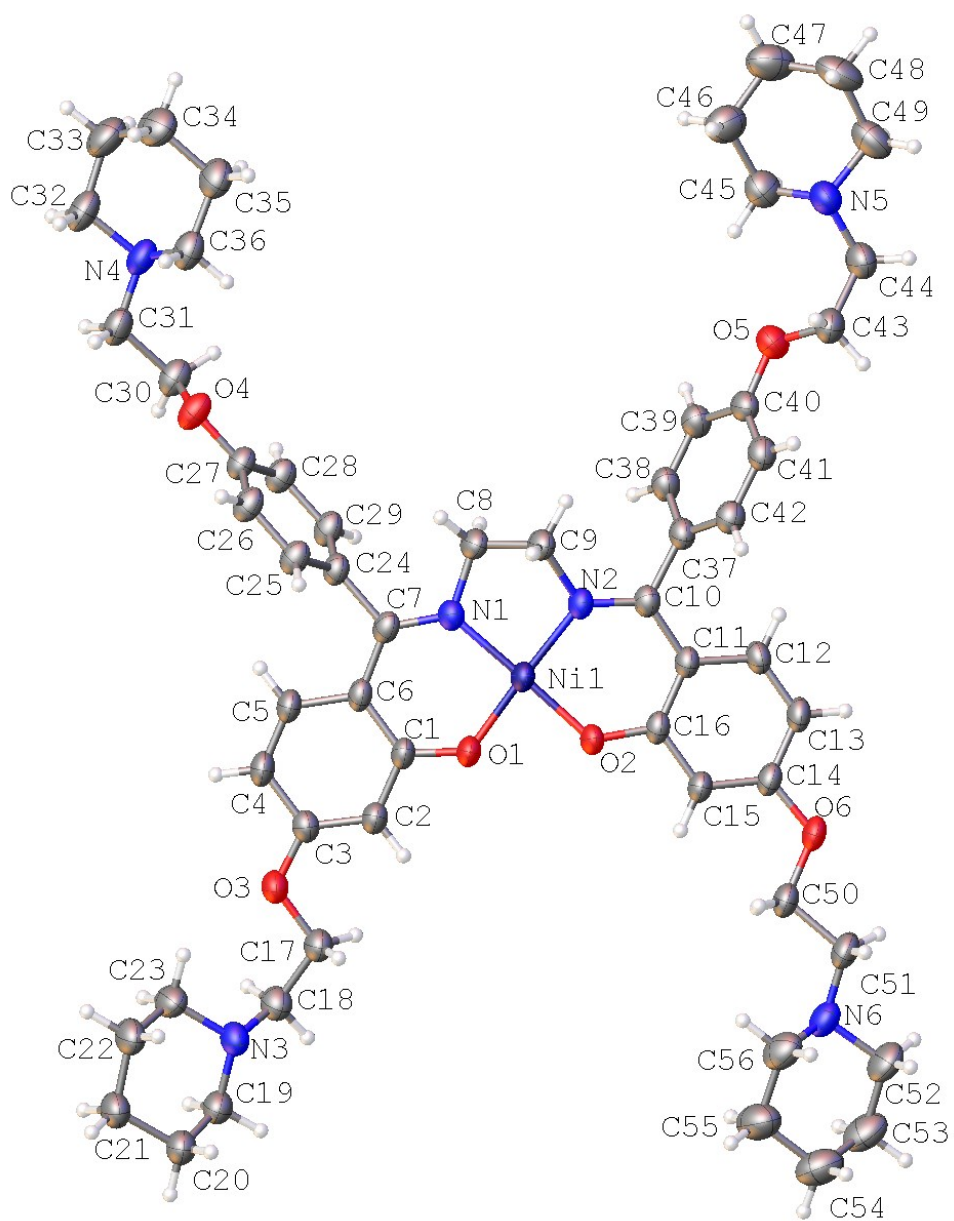


**Figure S9** The asymmetric unit of complex **(14)**.

**Table S11** Selected bond lengths (Å), bond angles (°) and average coplanar ring angles (°) for complexes **(5)**, **(7)**, **(9)**, and **(13)**.

	<b>(5)</b>	<b>(7)</b>	<b>(9)<sup>a</sup></b>	<b>(13)</b>
Ni-O1	1.8434(12)	1.8385(9)	1.8487(14)	1.8419(12)
Ni-O2	1.8232(13)	1.8313(9)	1.8360(14)	1.8401(12)
Ni-N1	1.8563(13)	1.8761(11)	1.8837(17)	1.8601(14)
Ni-N2	1.8541(16)	1.8944(12)	1.8873(18)	1.8523(15)
O1-Ni-O2	83.37(6)	82.72(4)	83.02(6)	83.15(5)
O2-Ni-N2	95.00(6)	92.48(5)	92.22(7)	94.84(6)
O1-Ni-N2	178.33(6)	171.65(5)	170.15(7)	176.27(6)
O2-Ni-N1	177.62(6)	171.67(5)	171.28(7)	175.28(6)
O1-Ni-N1	94.55(6)	92.46(5)	93.21(7)	94.28(6)
N1-Ni-N2	87.09(7)	93.08(5)	92.65(8)	87.95(6)
Ring A/Ring B	4	13	15	5
Ring A/Ring C	3	10	10	2
Ring B/Ring D	2	10	8	4
Ring C/Ring E	87	80	70	75
Ring D/Ring F	87	74	89	86

<sup>a</sup> for **(9)**: O1 = O16, O2 = O16P, N1 = N2, N2 = N2P.

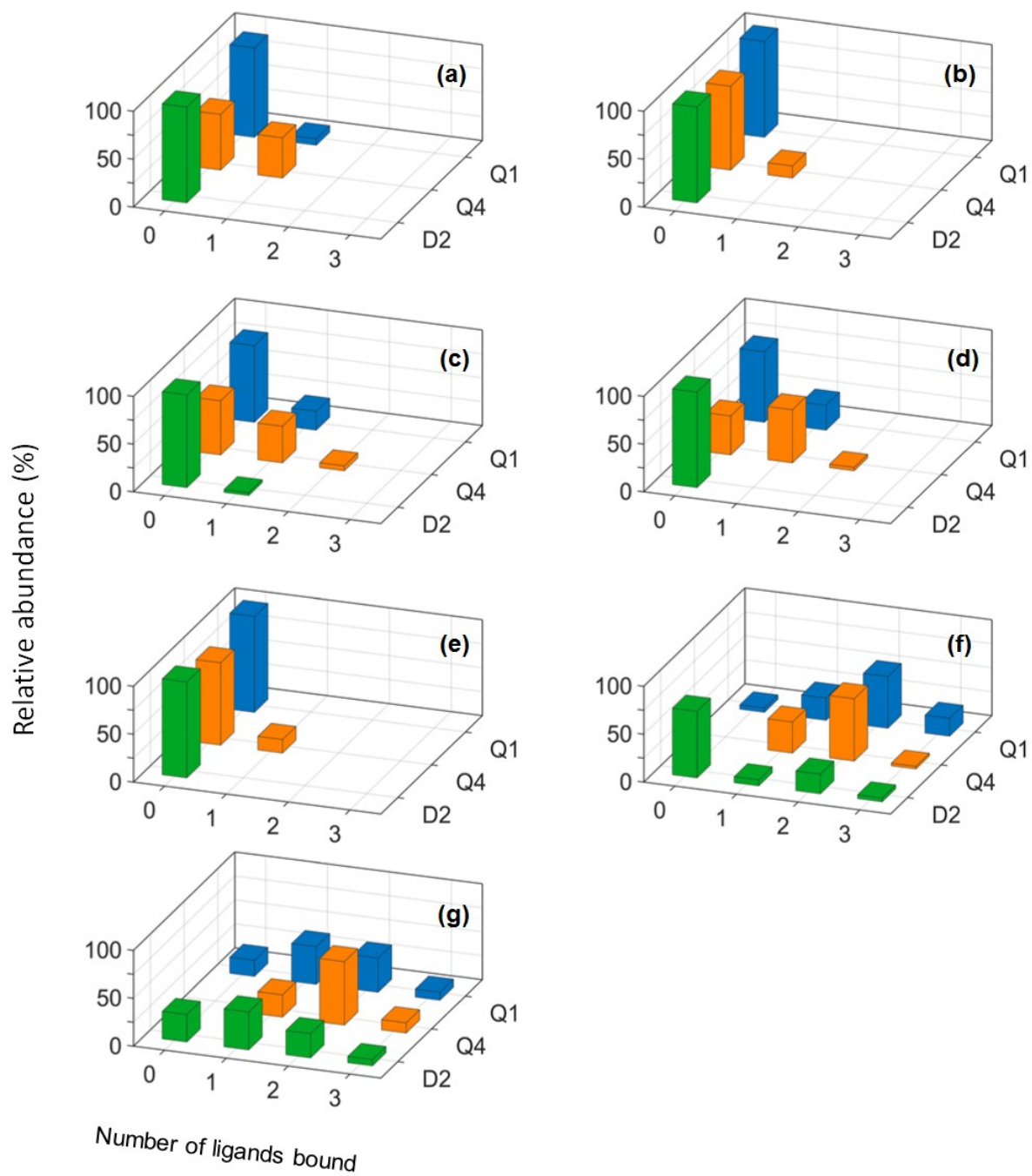


**Figure S10** Relative abundances of ions in ESI mass spectra of solutions containing a 6:1 ratio of nickel Schiff base complexes and dsDNA (D2), unimolecular G4-DNA (Q1) or tetramolecular G4-DNA (Q4): (a) solutions containing **(4)**; (b) solutions containing **(6)**; (c) solutions containing **(8)**; (d) solutions containing **(10)**; (e) solutions containing **(12)**; (f) solutions containing **(14)** and (g) solutions containing **(1)**.

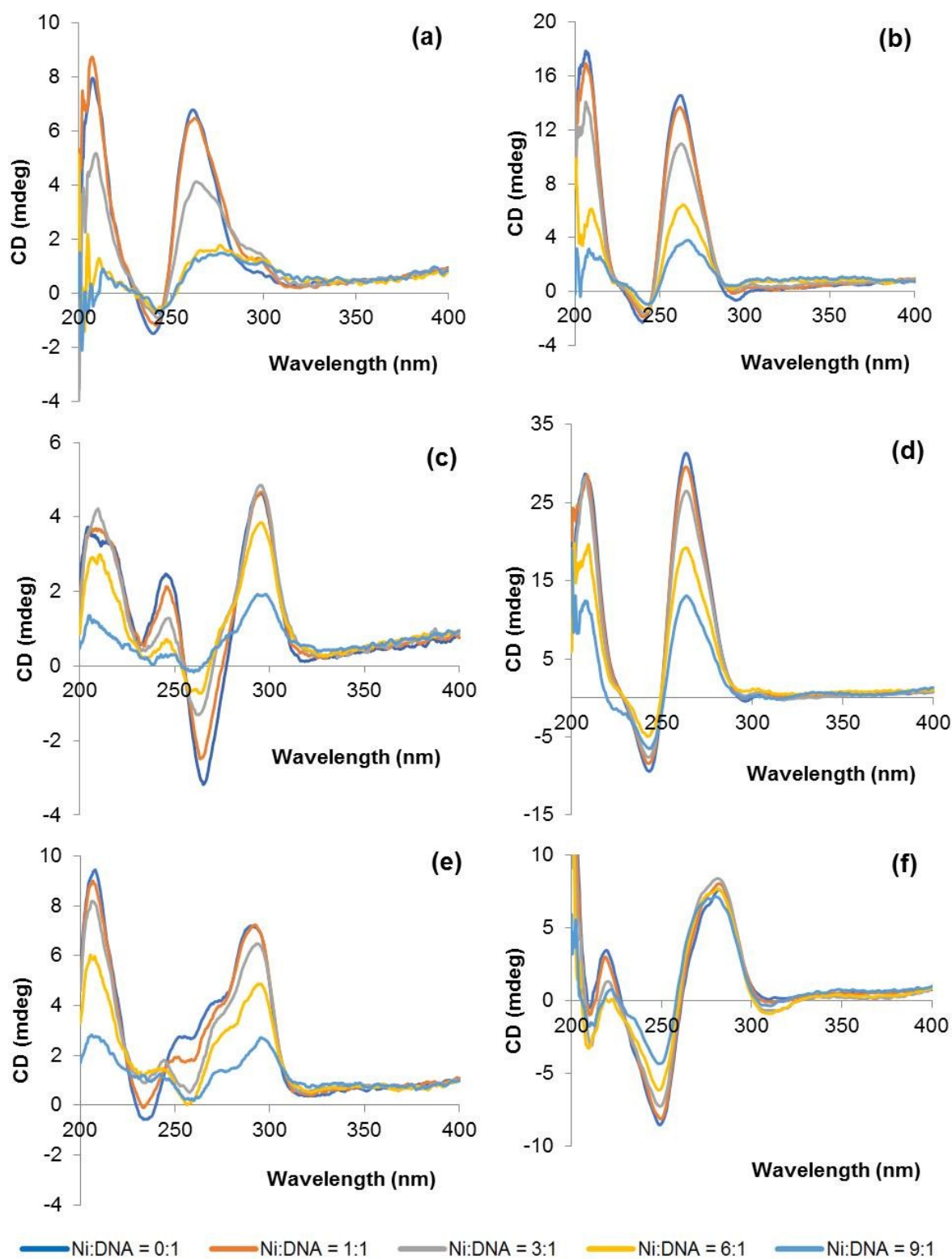


**Figure S11** Circular dichroism spectra of solutions containing different ratios of **(1)** and various DNA: (a) Parallel Q1 + **(1)**; (b) Parallel c-kit1 + **(1)**; (c) Anti-parallel Q1 + **(1)**; (d) Parallel Q4 + **(1)**; (e) Hybrid-type 1 Q1 + **(1)**; (f) D2 + **(1)**.

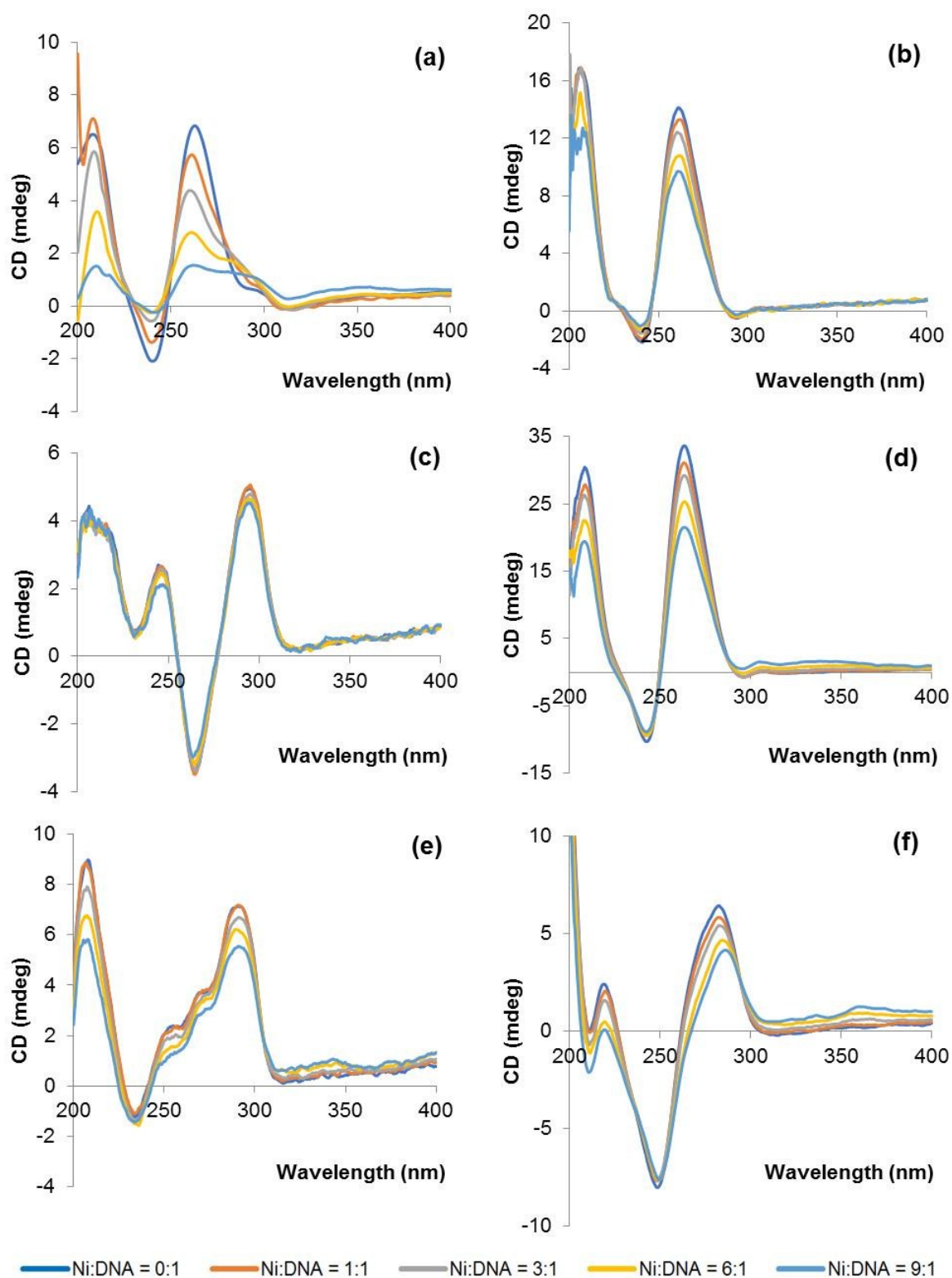


**Figure S12** Circular dichroism spectra of solutions containing different ratios of **(4)** and various DNA: (a) Parallel Q1 + **(4)**; (b) Parallel c-kit1 + **(4)**; (c) Anti-parallel Q1 + **(4)**; (d) Parallel Q4 + **(4)**; (e) Hybrid-type 1 Q1 + **(4)**; (f) D2 + **(4)**.

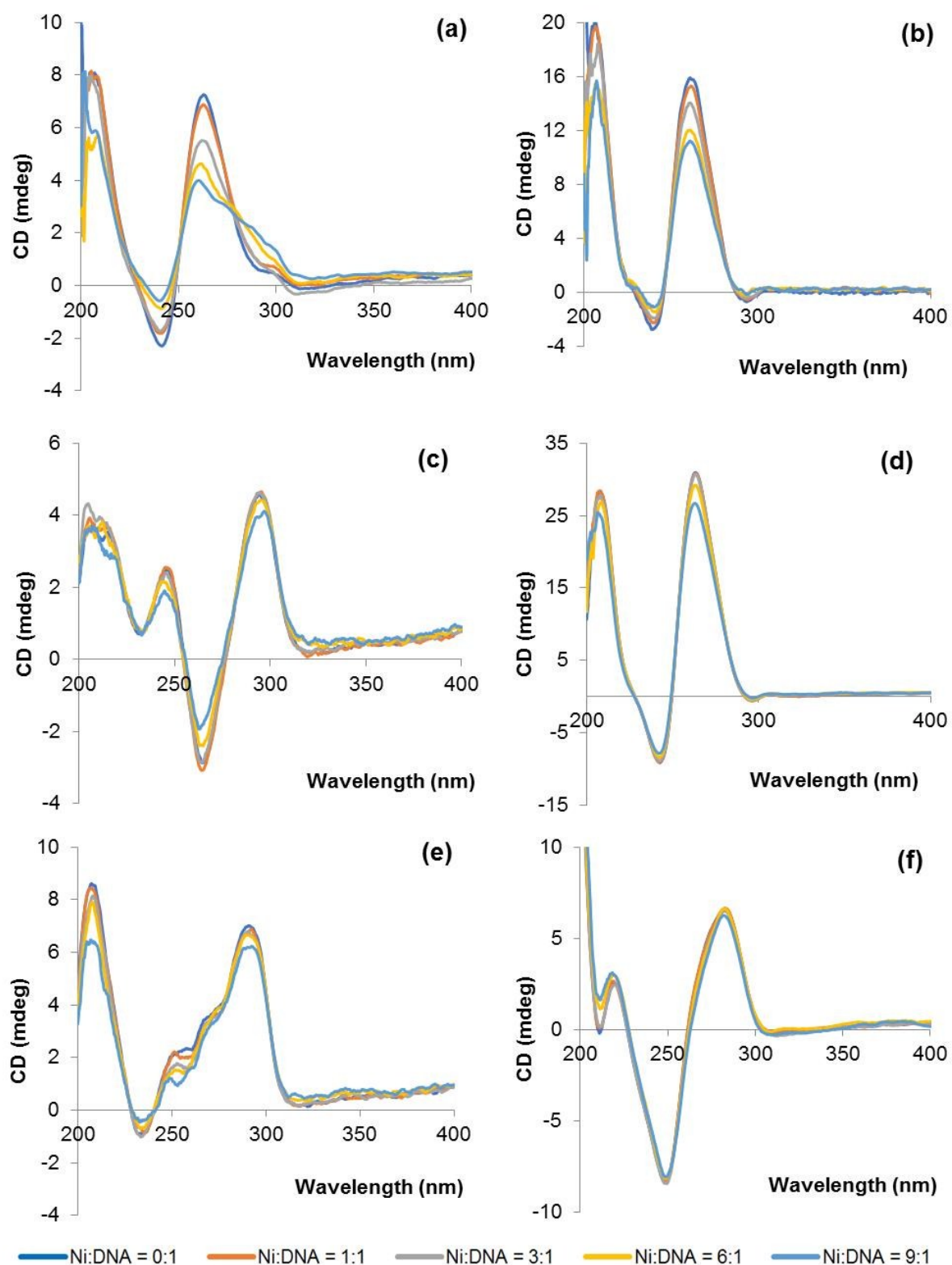


**Figure S13** Circular dichroism spectra of solutions containing different ratios of **(6)** and various DNA: (a) Parallel Q1 + **(6)**; (b) Parallel c-kit1 + **(6)**; (c) Anti-parallel Q1 + **(6)**; (d) Parallel Q4 + **(6)**; (e) Hybrid-type 1 Q1 + **(6)**; (f) D2 + **(6)**.

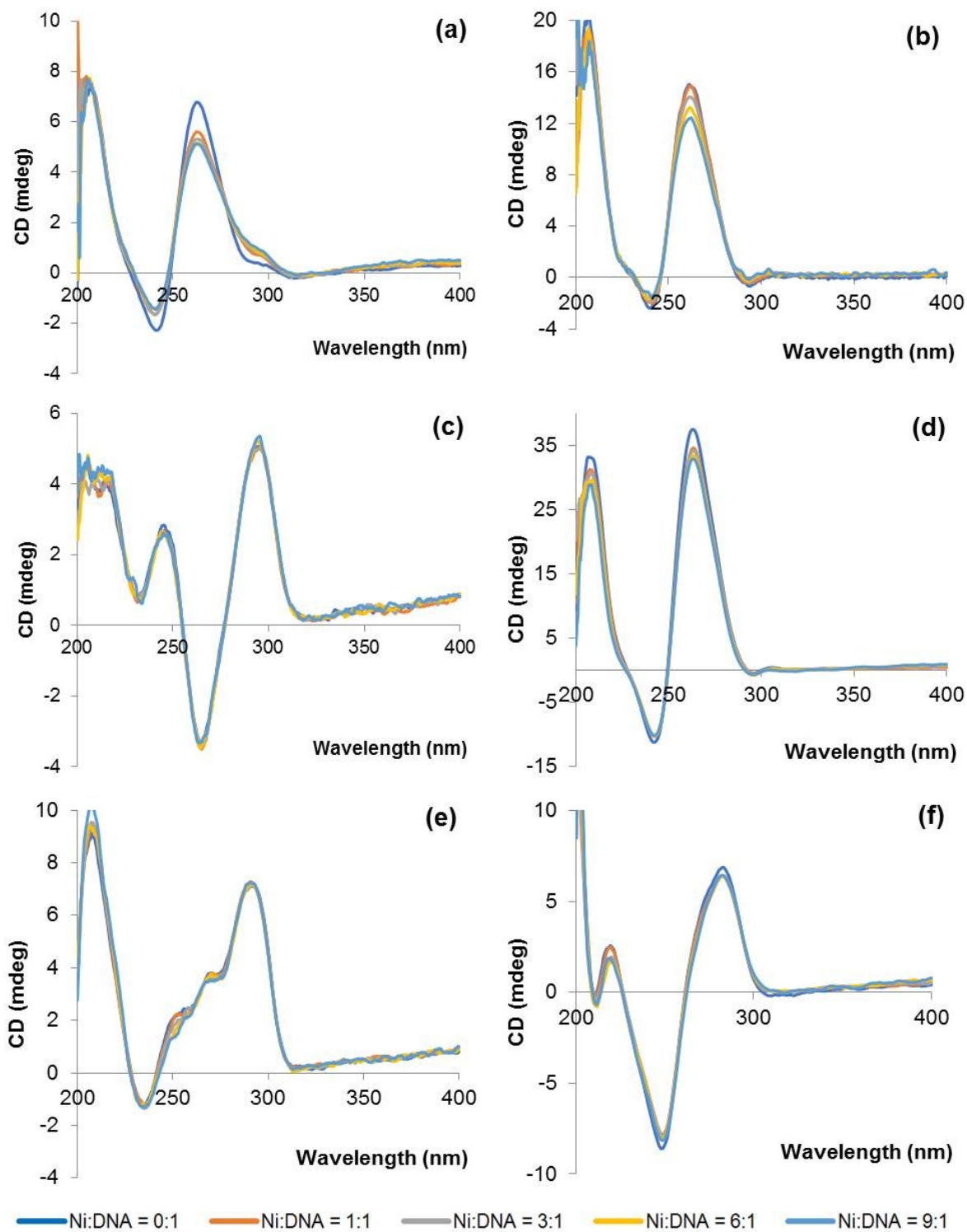


**Figure S14** Circular dichroism spectra of solutions containing different ratios of **(8)** and various DNA: (a) Parallel Q1 + **(8)**; (b) Parallel c-kit1 + **(8)**; (c) Anti-parallel Q1 + **(8)**; (d) Parallel Q4 + **(8)**; (e) Hybrid-type 1 Q1 + **(8)**; (f) D2 + **(8)**.

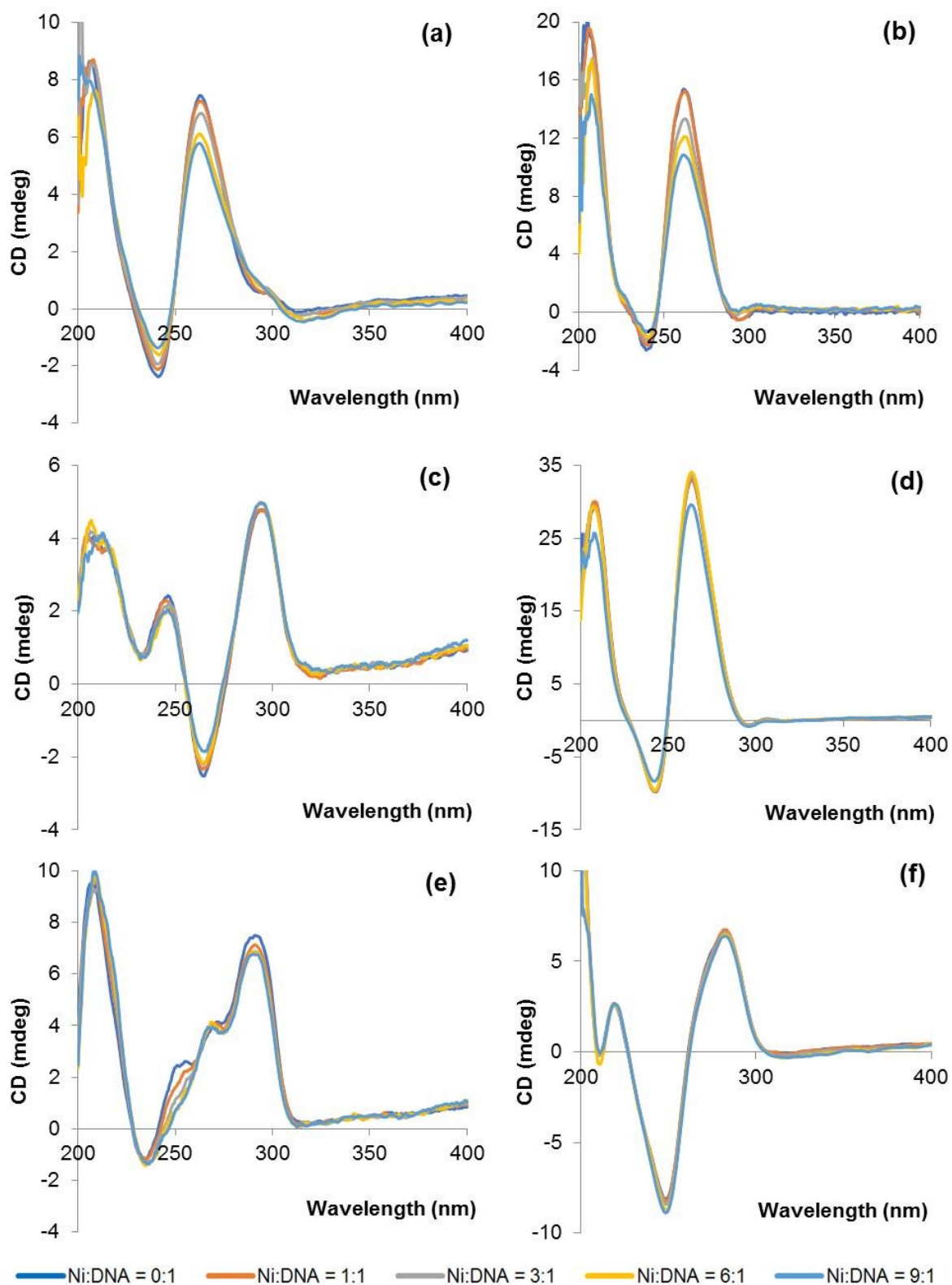


**Figure S15** Circular dichroism spectra of solutions containing different ratios of **(10)** and various DNA: (a) Parallel Q1 + **(10)**; (b) Parallel c-kit1 + **(10)**; (c) Anti-parallel Q1 + **(10)**; (d) Parallel Q4 + **(10)**; (e) Hybrid-type 1 Q1 + **(10)**; (f) D2 + **(10)**.

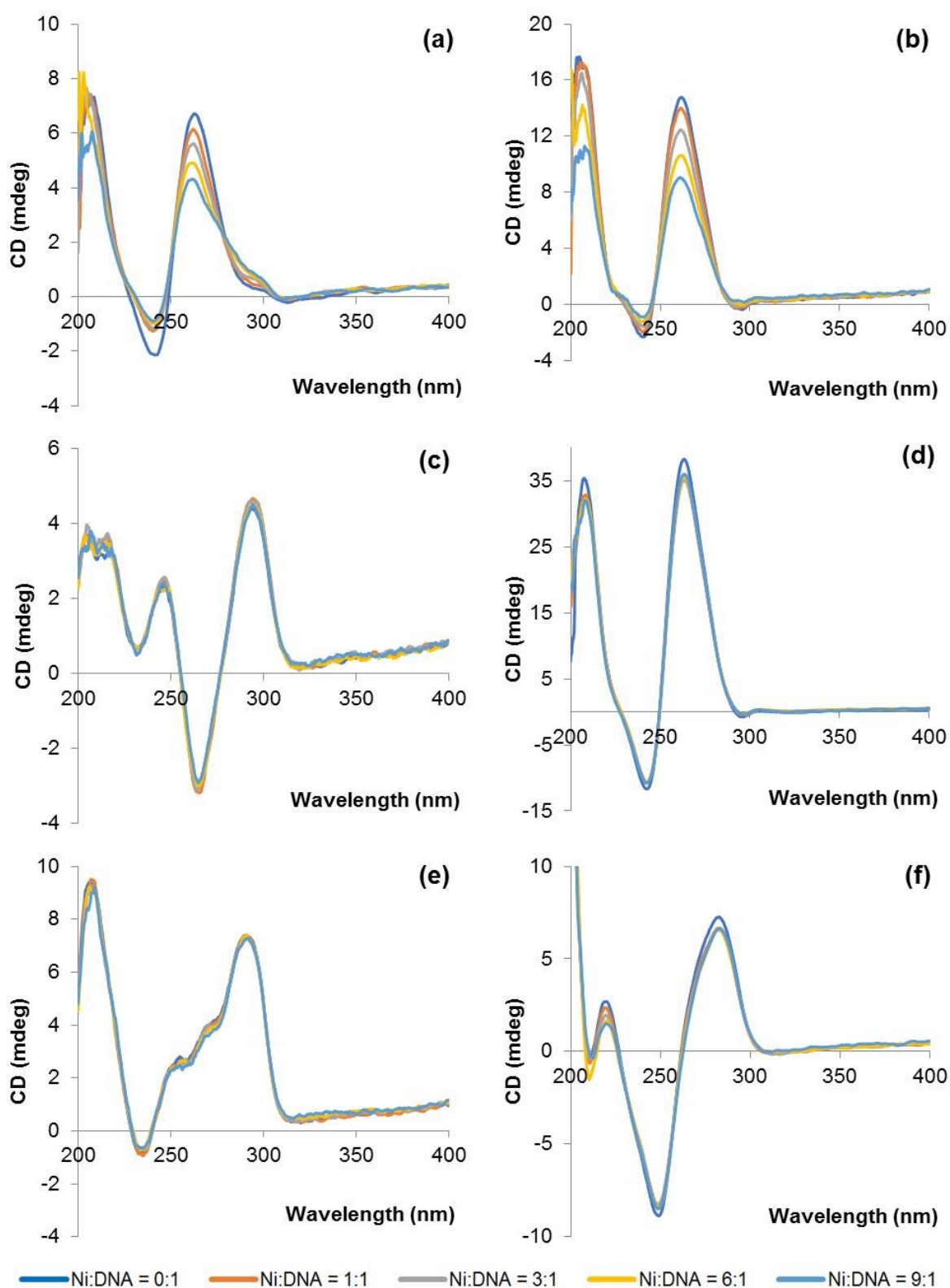


**Figure S16** Circular dichroism spectra of solutions containing different ratios of **(12)** and various DNA: (a) Parallel Q1 + **(12)**; (b) Parallel c-kit1 + **(12)**; (c) Anti-parallel Q1 + **(12)**; (d) Parallel Q4 + **(12)**; (e) Hybrid-type 1 Q1 + **(12)**; (f) D2 + **(12)**.

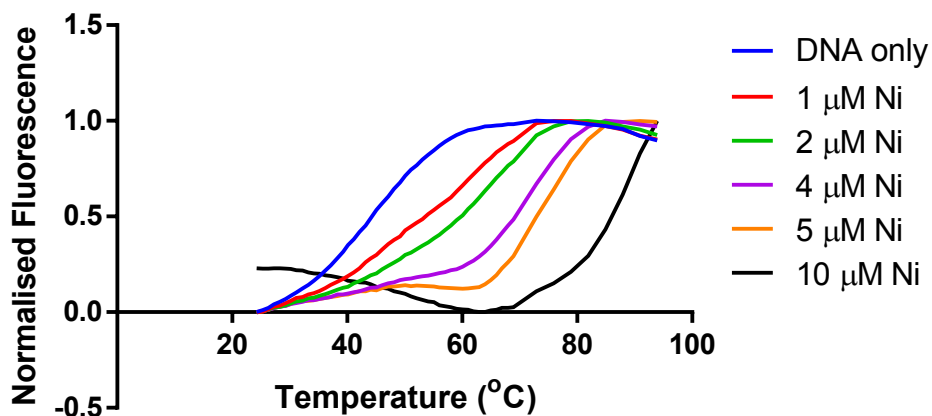


**Figure S17** Normalised FRET melting curves obtained using solutions containing 0.2  $\mu\text{M}$  F21T and different concentrations of **(1)**.

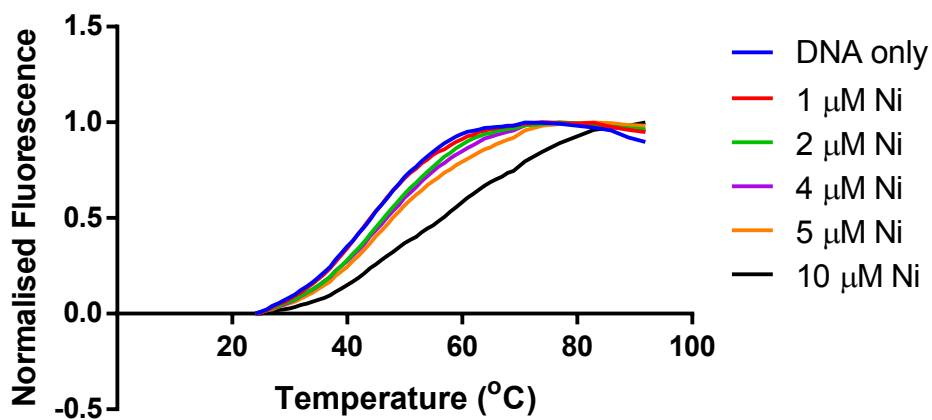


**Figure S18** Normalised FRET melting curves obtained using solutions containing 0.2  $\mu\text{M}$  F21T and different concentrations of **(4)**.

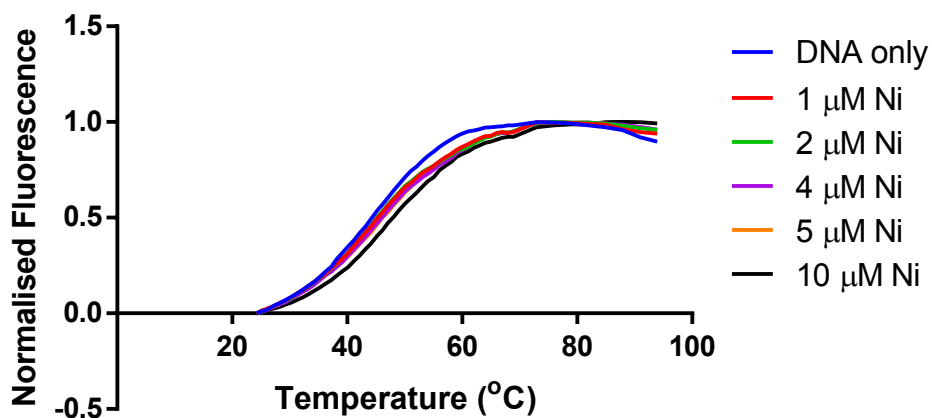


**Figure S19** Normalised FRET melting curves obtained using solutions containing 0.2  $\mu\text{M}$  F21T and different concentrations of **(6)**.

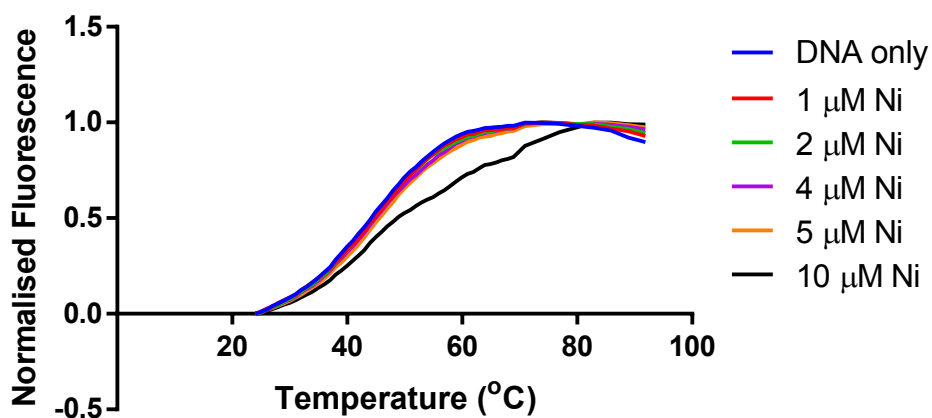


**Figure S20** Normalised FRET melting curves obtained using solutions containing 0.2  $\mu\text{M}$  F21T and different concentrations of **(8)**.

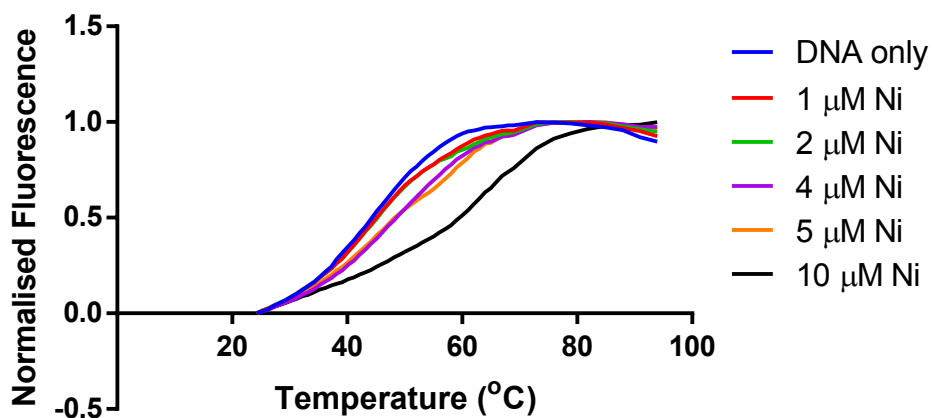


**Figure S21** Normalised FRET melting curves obtained using solutions containing 0.2 µM F21T and different concentrations of **(10)**.

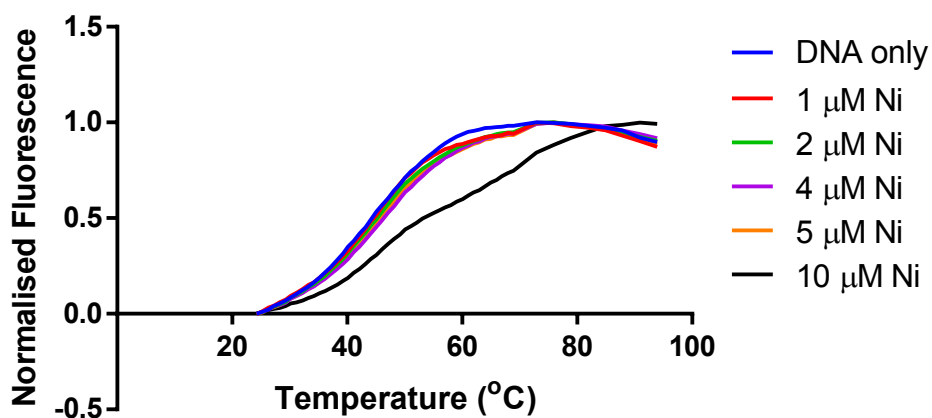


**Figure S22** Normalised FRET melting curves obtained using solutions containing 0.2 µM F21T and different concentrations of **(12)**.

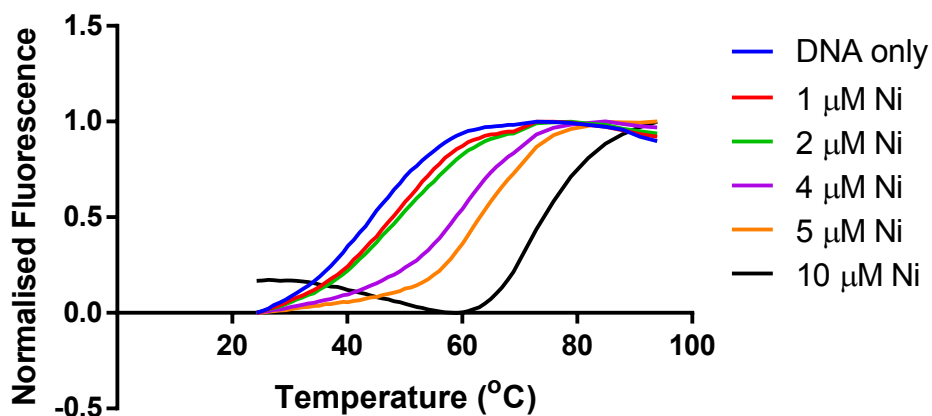


**Figure S23** Normalised FRET melting curves obtained using solutions containing 0.2 μM F21T and different concentrations of **(14)**.

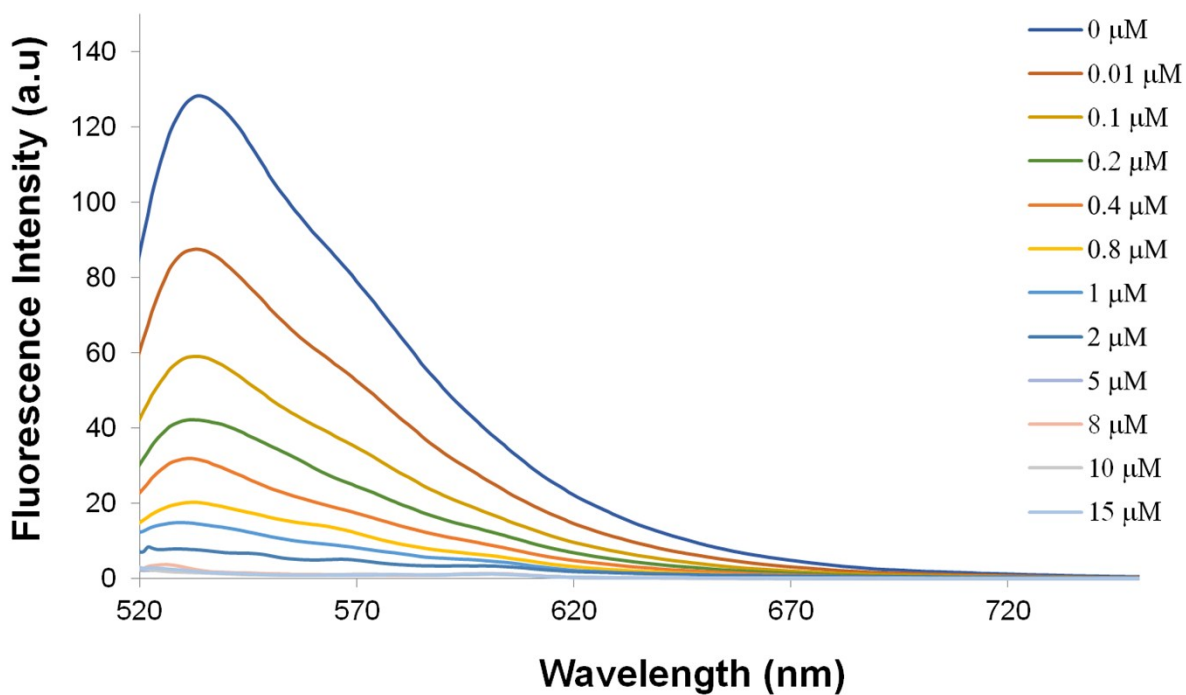


**Figure S24** Fluorescence spectra for solution containing Q1 and TO upon addition of increasing amounts of complex **(1)**.

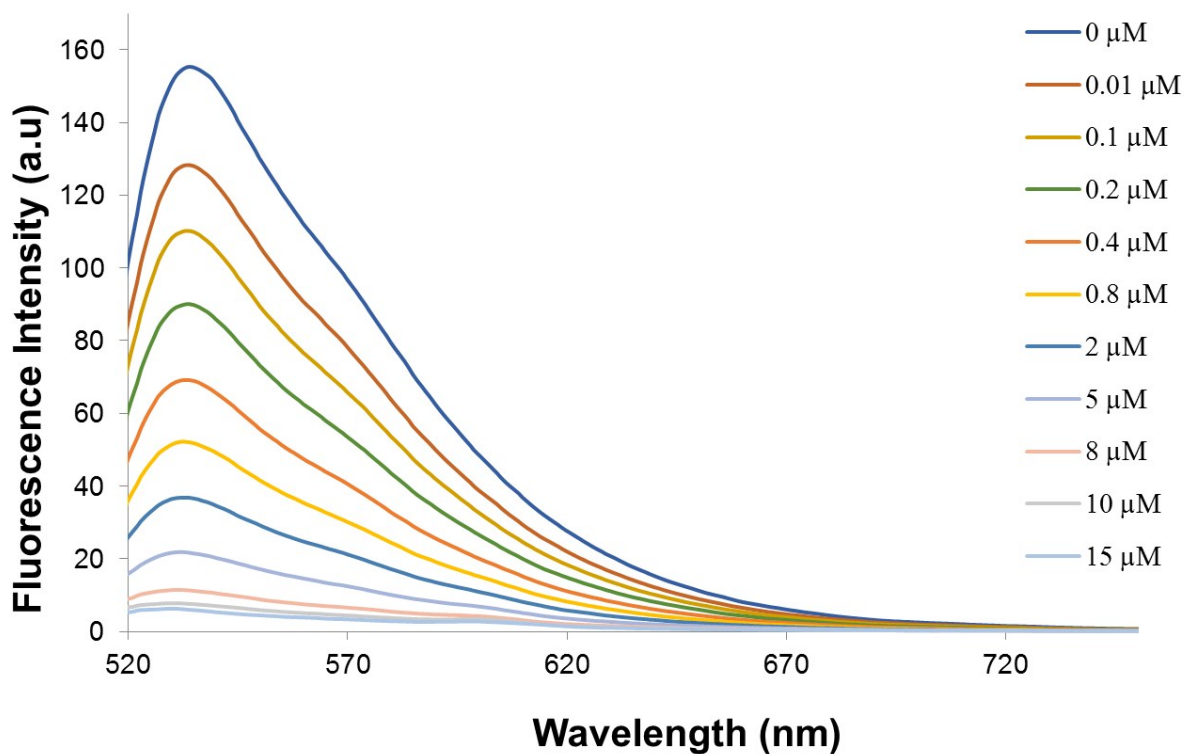


**Figure S25** Fluorescence spectra for solution containing Q1 and TO upon addition of increasing amounts of complex (4).

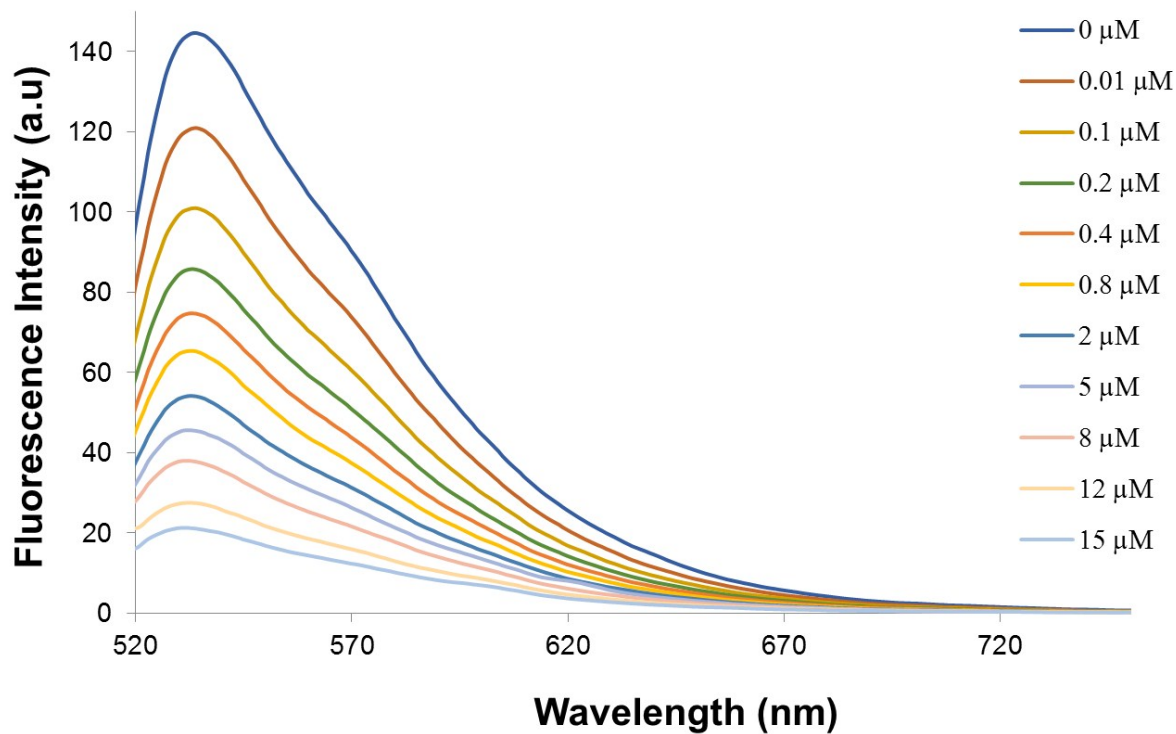


**Figure S26** Fluorescence spectra for solution containing Q1 and TO upon addition of increasing amounts of complex (6).

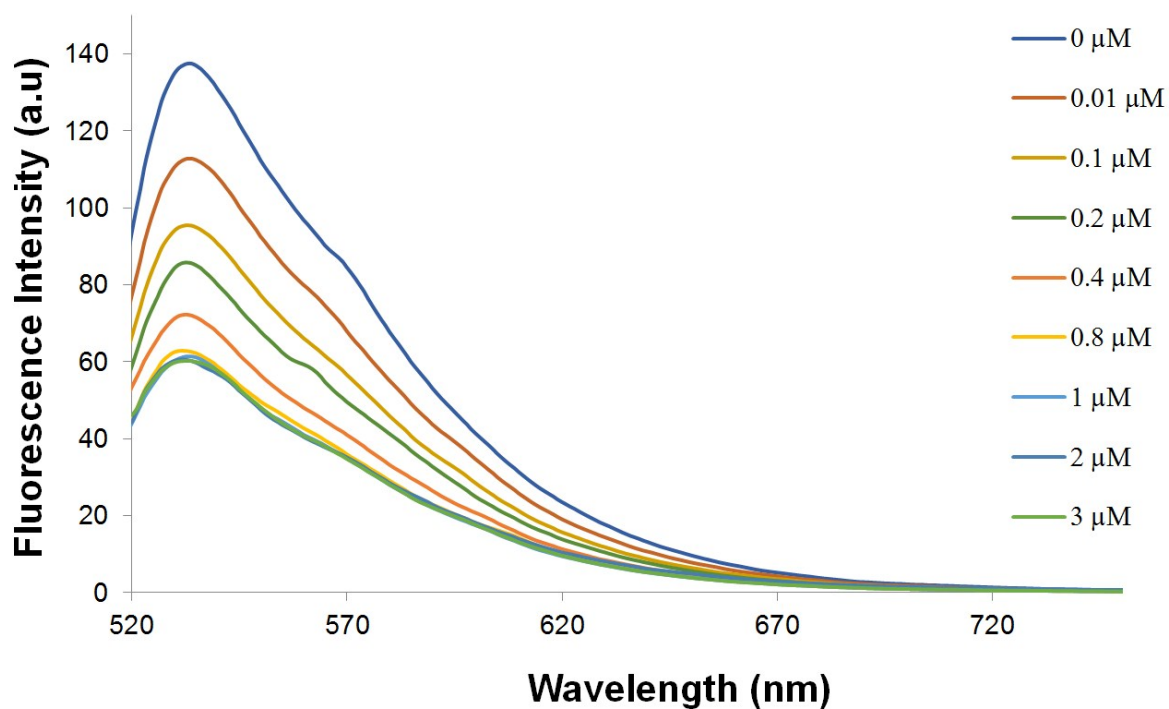


**Figure S27** Fluorescence spectra for solution containing Q1 and TO upon addition of increasing amounts of complex (8).

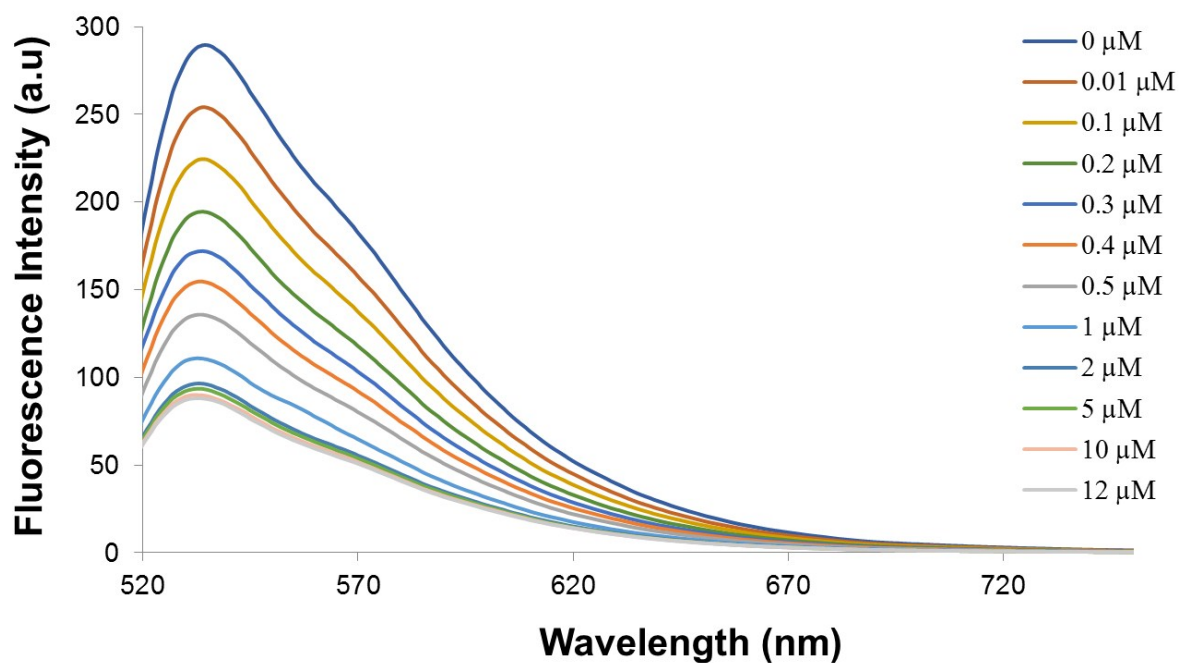


**Figure S28** Fluorescence spectra for solution containing Q1 and TO upon addition of increasing amounts of complex (10).

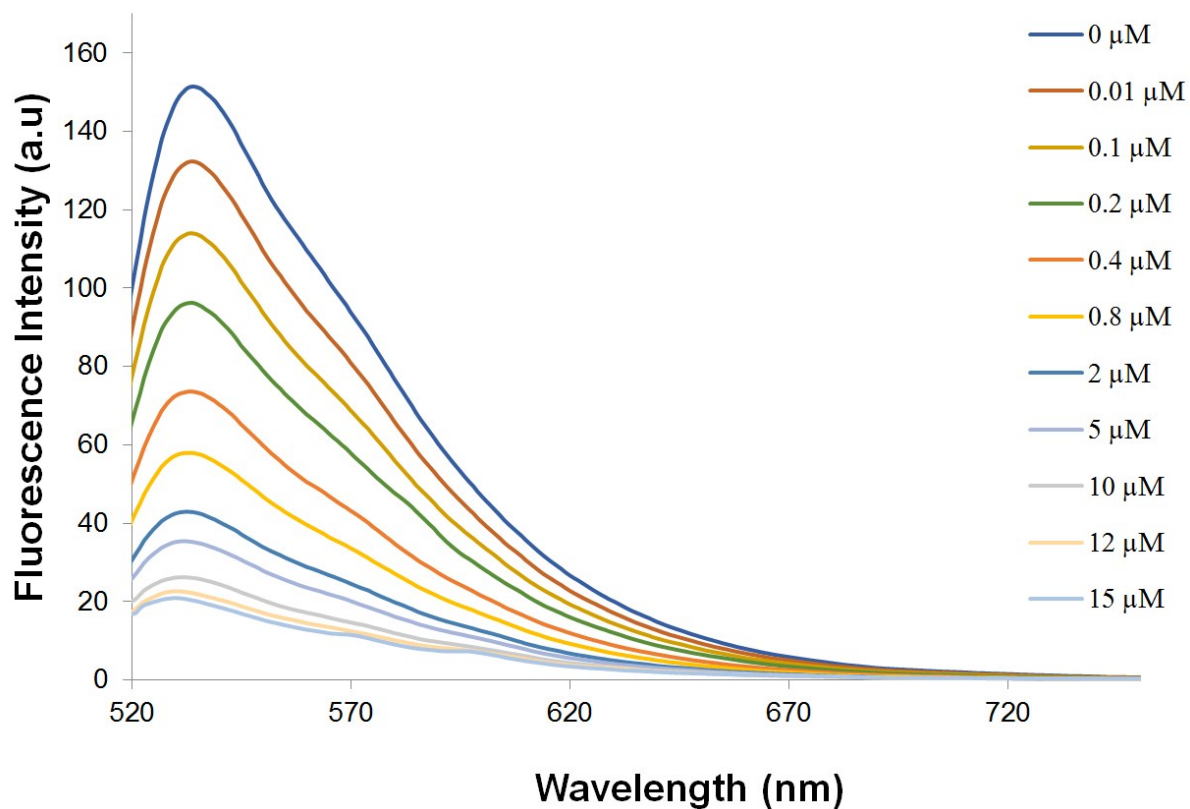


**Figure S29** Fluorescence spectra for solution containing Q1 and TO upon addition of increasing amounts of complex **(12)**.

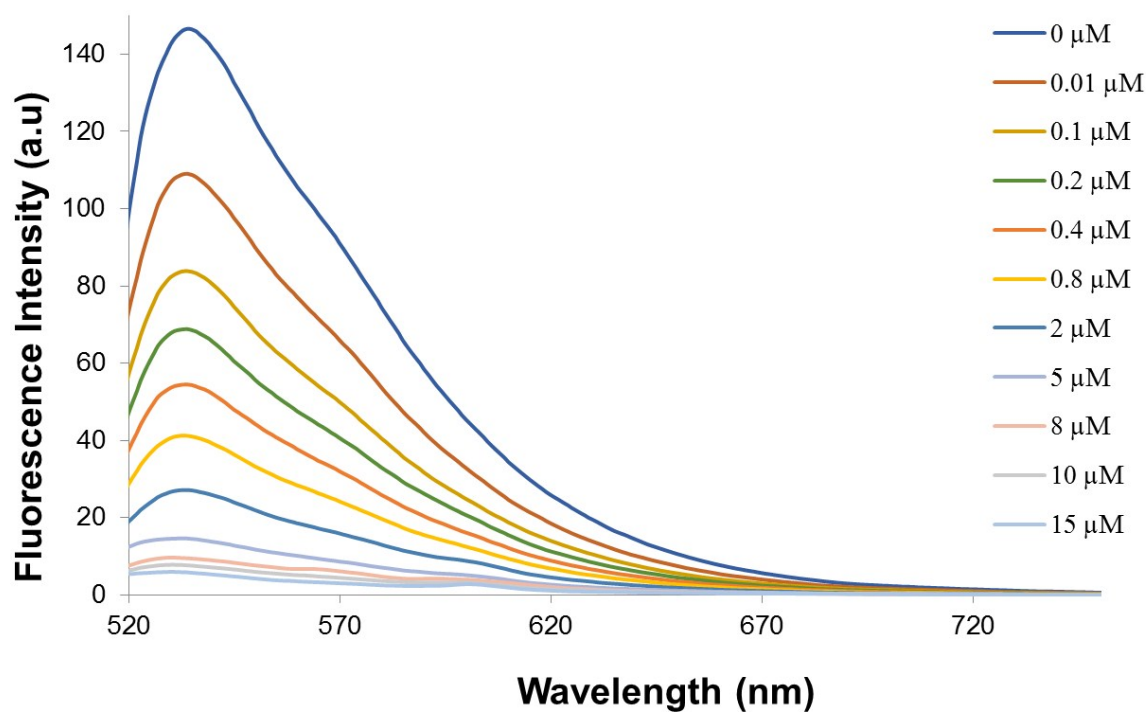


**Figure S30** Fluorescence spectra for solution containing Q1 and TO upon addition of increasing amounts of complex **(14)**.



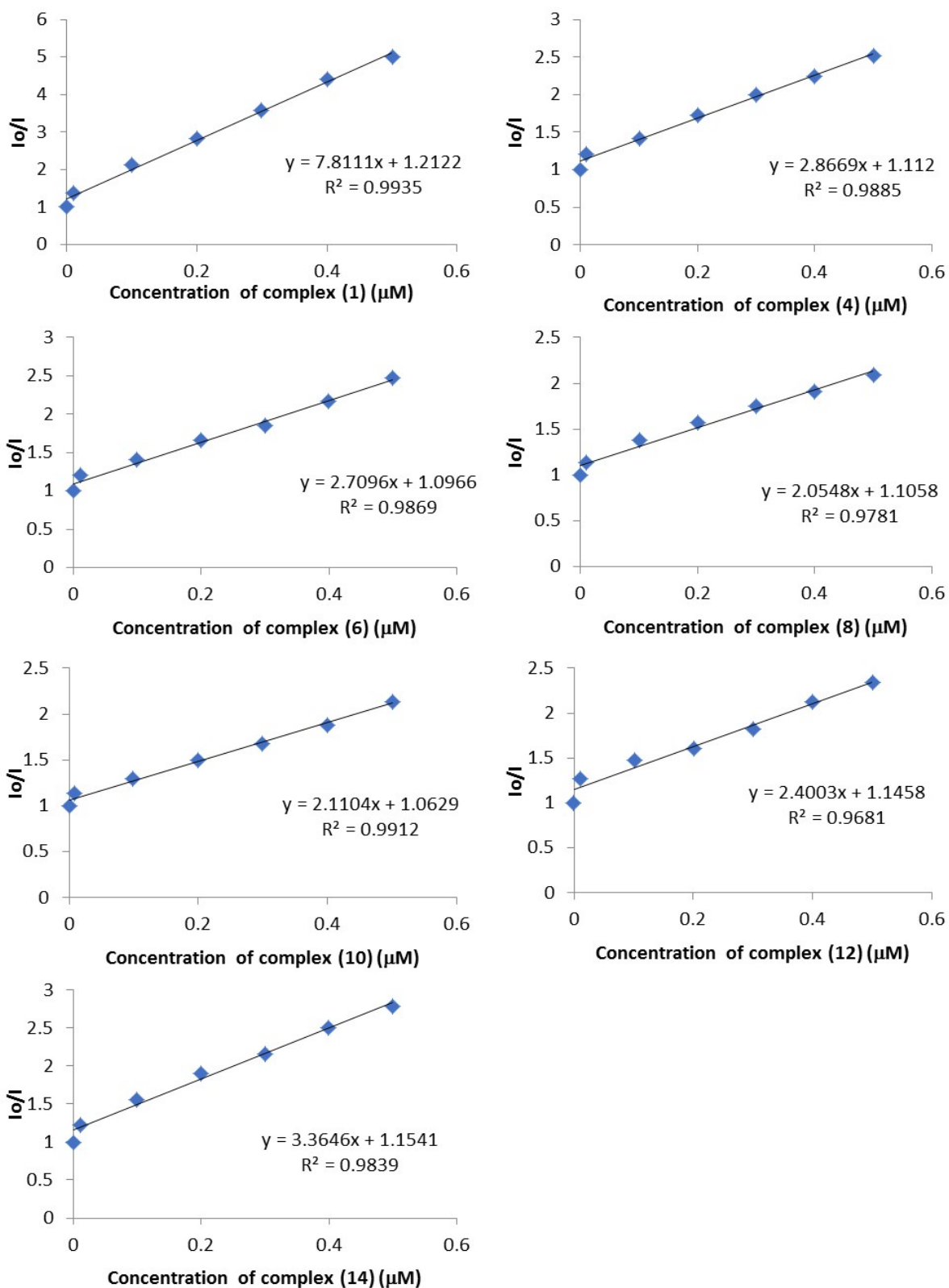


**Figure S31** Stern-Volmer plots for FID assays of complexes (1), (4), (6), (8), (10), (12) and (14) using Q1 and TO.

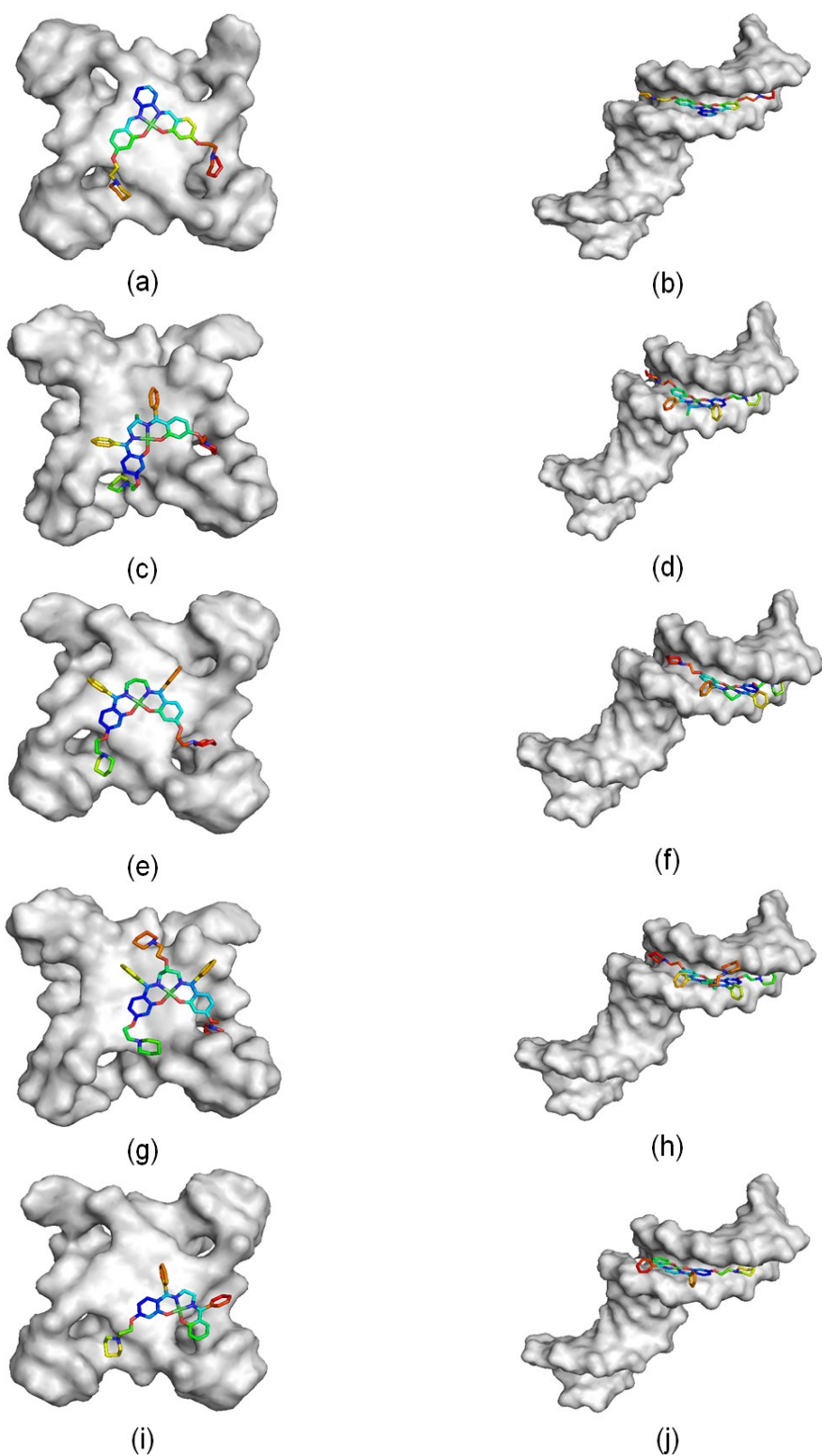


**Figure S32** Molecular docking configurations of complex **(1)**, **(6)**, **(8)**, **(10)** and **(12)** with the 22AG qDNA (1KF1) and dsDNA (1KBD): (a) **(1)** and 1KF1; (b) **(1)** and 1KBD; (c) **(6)** and 1KF1; (d) **(6)** and 1KBD; (e) **(8)** and 1KF1; (f) **(8)** and 1KBD; (g) **(10)** and 1KF1; (h) **(10)** and 1KBD; (i) **(12)** and 1KF1; (j) **(12)** and 1KBD.

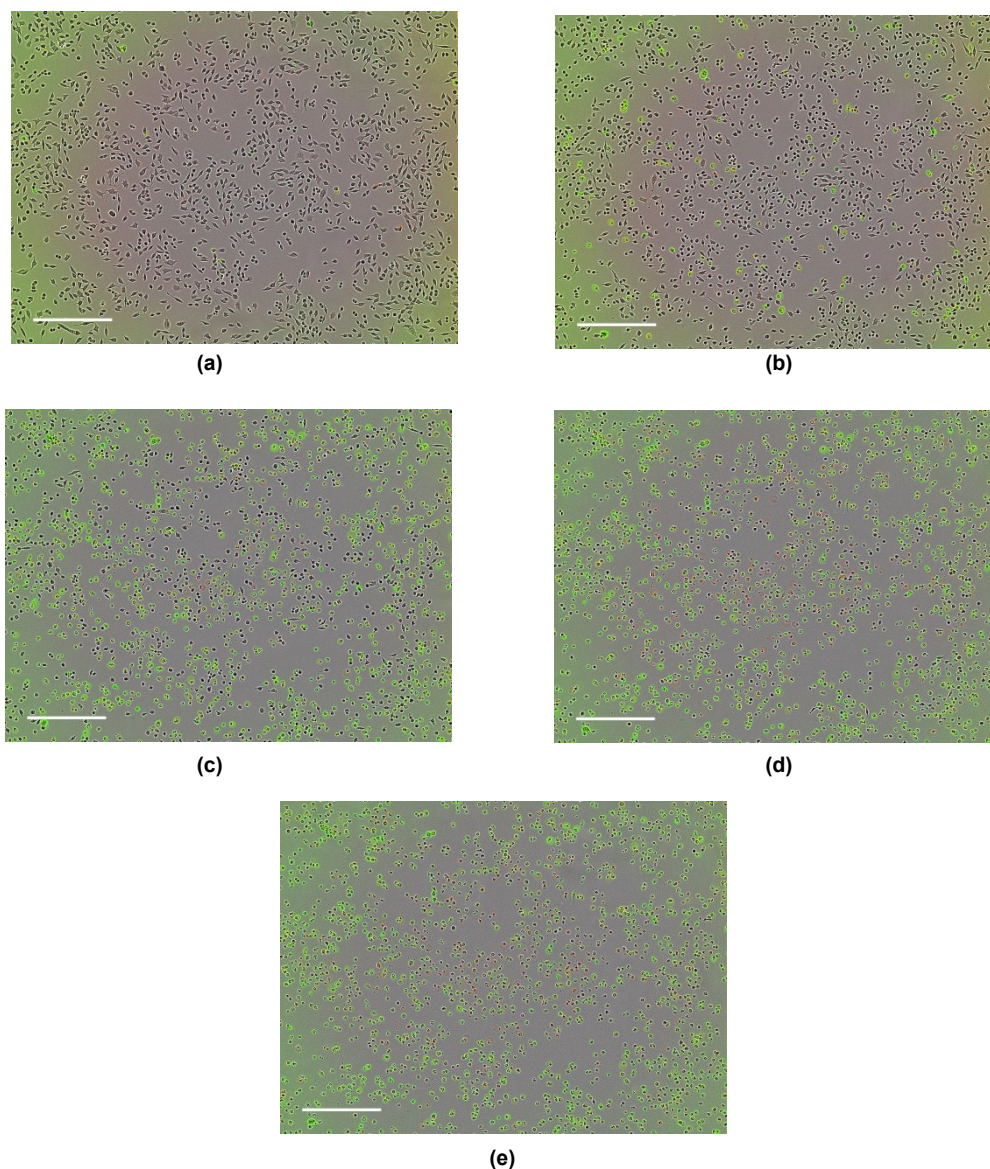


**Figure S33** Images obtained from time course fluorescence experiments performed using of V79 cells. All images were obtained using 10x magnification. The cells were treated with 5  $\mu\text{M}$  (**4**), and then images obtained every 6 h over a 24 h time period: (a) image obtained 0 h from the time of complex administration; (b) 6 h; (c) 12 h; (d) 18 h; (e) 24 h. Green corresponds to cells exhibiting fluorescence from AnnexinVFITC, while red corresponds to fluorescence from 7AAD. Scale bar indicates 300  $\mu\text{m}$ .

#### Notes and references

1. Altomare A., Cascarano G., Giacobazzo G., Guagliardi A., Burla M.C., Polidori G., and Camalli M., *J. Appl. Crystallogr.*, 1994. **27**: p. 435-435.
2. Betteridge P.W., Carruthers J.R., Cooper R.I., Prout K., and Watkin D.J., *J. Appl. Crystallogr.*, 2003. **36**: p. 1487-1487.
3. Sheldrick G.M., *Acta Cryst. A*, 2015. **71**(1): p. 3-8.
4. Sheldrick G.M., *Acta. Crystallogr. C. Struct. Chem.*, 2015. **71**(Pt 1): p. 3-8.
5. Dolomanov O.V., Bourhis L.J., Gildea R.J., Howard J.A.K., and Puschmann H., *J. Appl. Crystallogr.*, 2009. **42**(2): p. 339-341.